RESEARCH ARTICLE

Fasting-Mimicking Diet Is Safe and Reshapes Metabolism and Antitumor Immunity in Patients with Cancer

Claudio Vernieri[1,2], Giovanni Fucà[1], Francesca Ligorio[1], Veronica Huber[3], Andrea Vingiani[4,5], Fabio Iannelli[2], Alessandra Raimondi[1], Darawan Rinchai[6], Gianmaria Frigè[7], Antonino Belfiore[5], Luca Lalli[3], Claudia Chiodoni[8], Valeria Cancila[9], Federica Zanardi[2], Arta Ajazi[2], Salvatore Cortellino[2], Viviana Vallacchi[3], Paola Squarcina[3], Agata Cova[3], Samantha Pesce[3], Paola Frati[3], Raghvendra Mall[10], Paola Antonia Corsetto[11], Angela Maria Rizzo[11], Cristina Ferraris[12], Secondo Folli[12], Marina Chiara Garassino[1], Giuseppe Capri[1], Giulia Bianchi[1], Mario Paolo Colombo[8], Saverio Minucci[7,13], Marco Foiani[2,4], Valter Daniel Longo[2,14], Giovanni Apolone[15], Valter Torri[16], Giancarlo Pruneri[4,5], Davide Bedognetti[6,17,18], Licia Rivoltini[3], and Filippo de Braud[1,4]

ABSTRACT In tumor-bearing mice, cyclic fasting or fasting-mimicking diets (FMD) enhance the activity of antineoplastic treatments by modulating systemic metabolism and boosting antitumor immunity. Here we conducted a clinical trial to investigate the safety and biological effects of cyclic, five-day FMD in combination with standard antitumor therapies. In 101 patients, the FMD was safe, feasible, and resulted in a consistent decrease of blood glucose and growth factor concentration, thus recapitulating metabolic changes that mediate fasting/FMD anticancer effects in preclinical experiments. Integrated transcriptomic and deep-phenotyping analyses revealed that FMD profoundly reshapes anticancer immunity by inducing the contraction of peripheral blood immunosuppressive myeloid and regulatory T-cell compartments, paralleled by enhanced intratumor Th1/cytotoxic responses and an enrichment of IFNγ and other immune signatures associated with better clinical outcomes in patients with cancer. Our findings lay the foundations for phase II/III clinical trials aimed at investigating FMD antitumor efficacy in combination with standard antineoplastic treatments.

SIGNIFICANCE: Cyclic FMD is well tolerated and causes remarkable systemic metabolic changes in patients with different tumor types and treated with concomitant antitumor therapies. In addition, the FMD reshapes systemic and intratumor immunity, finally activating several antitumor immune programs. Phase II/III clinical trials are needed to investigate FMD antitumor activity/efficacy.

INTRODUCTION

In tumor-bearing mice, cyclic fasting or calorie-restricted, low-carbohydrate, low-protein diets, collectively referred to as fasting-mimicking diets (FMD), have convincingly demonstrated additive or synergistic antitumor activity in combination with cytotoxic chemotherapy (ChT), immunotherapy, or endocrine therapies (1–6). These anticancer effects are mostly mediated by fasting/FMD-induced reduction of blood glucose, insulin, and insulin-like growth factor 1 (IGF1) concentration, which results in the inhibition of anabolic processes that sustain unrestrained growth/proliferation and the repair of chemotherapy-induced genotoxic and proteotoxic effects in cancer cells (2, 6). More recently, fasting and FMD were shown to boost tumor infiltration by $CD8^+$ T cells—the effectors of antitumor immune responses—and to reduce immunosuppressive regulatory T cells (Treg) in syngeneic mouse models (3, 5).

On the basis of this preclinical evidence, clinical trials have been initiated to investigate the feasibility and antitumor activity of cyclic FMD in combination with standard antitumor therapies in different clinical contexts (NCT03709147, NCT04248998, NCT03700437). The only study whose results have been reported so far is the phase II trial "DIRECT" (NCT02126449), which was prematurely interrupted because of poor patient compliance with the proposed FMD regimen and because the FMD failed to reduce ChT-induced adverse events (7).

Here we report on the final results of a first-in-human clinical trial (NCT03340935) that investigated the safety, feasibility, and metabolic and immunomodulatory effects of a severely calorie-restricted, five-day FMD regimen in patients with cancer. We also report on results of an interim analysis in which we investigated FMD-induced systemic and intratumor immune responses in 22 patients with breast cancer enrolled in the ongoing DigesT trial (NCT03454282).

[1]Medical Oncology Department, Fondazione IRCCS Istituto Nazionale dei Tumori, Milan, Italy. [2]IFOM, The FIRC Institute of Molecular Oncology, Milan, Italy. [3]Unit of Immunotherapy of Human Tumors, Fondazione IRCCS Istituto Nazionale dei Tumori, Milan, Italy. [4]Oncology and Haemato-Oncology Department, University of Milan, Milan, Italy. [5]Deparment of Pathology and Laboratory Medicine, Fondazione IRCCS Istituto Nazionale dei Tumori, Milan, Italy. [6]Immunology Department, Cancer Program, Sidra Medicine, Doha, Qatar. [7]Department of Experimental Oncology, European Institute of Oncology (IEO), IRCCS, Milan, Italy. [8]Molecular Immunology Unit, Fondazione IRCCS Istituto Nazionale dei Tumori, Milan, Italy. [9]Tumor Immunology Unit, Department of Health Sciences, University of Palermo, Palermo, Italy. [10]Qatar Computing Research Institute, Hamad Bin Khalifa University, Doha, Qatar. [11]Department of Pharmacological and Biomolecular Sciences, University of Milan, Milan, Italy. [12]Breast Unit, Fondazione IRCCS Istituto Nazionale dei Tumori. Milan 20133, Italy. [13]Department of Biosciences, University of Milan, Milan, Italy. [14]Longevity Institute, School of Gerontology, Department of Biological Sciences, University of Southern California, Los Angeles, California. [15]Scientific Directorate, Fondazione IRCCS Istituto Nazionale dei Tumori. Milan, Italy. [16]Laboratory of Methodology for Biomedical Research, Istituto di Ricerche Farmacologiche "Mario Negri" IRCCS, Milan, Italy. [17]Dipartimento di Medicina Interna e Specialità Mediche, Università degli Studi di Genova, Genova, Italy. [18]College of Health and Life Sciences, Hamad Bin Khalifa University, Doha, Qatar.

Note: Supplementary data for this article are available at Cancer Discovery Online (http://cancerdiscovery.aacrjournals.org/).

D. Bedognetti, L. Rivoltini, and F. de Braud contributed equally to this article.

Corresponding Authors: Claudio Vernieri, IFOM, The FIRC Institute of Molecular Oncology and Fondazione IRCCS Istituto Nazionale dei Tumori, Milan, Italy. Phone: 390223903066; E-mail: claudio.vernieri@istitutotumori.mi.it or claudio.vernieri@ifom.eu; and Licia Rivoltini, licia.rivoltini@istitutotumori.mi.it

Cancer Discov 2022;12:90–107

doi: 10.1158/2159-8290.CD-21-0030

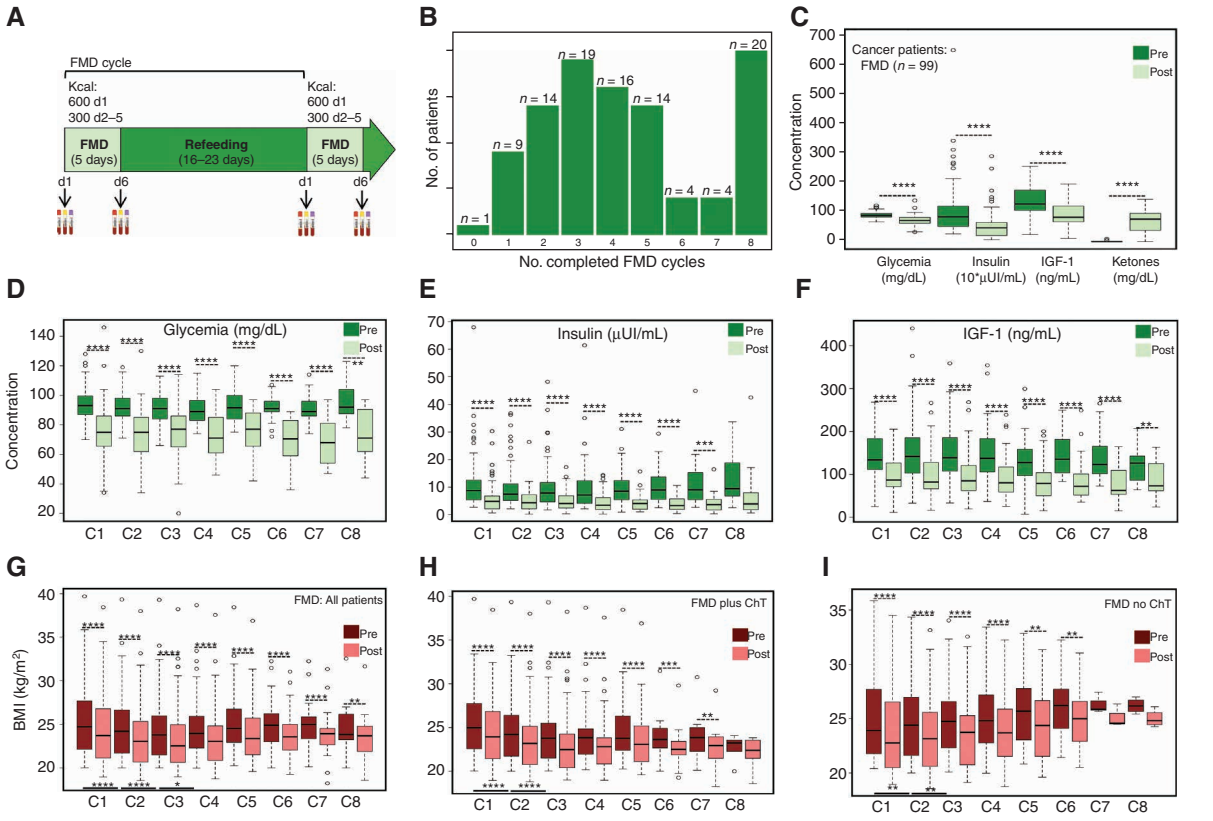

Figure 1. The fasting-mimicking diet (FMD) reduces blood glucose and growth factor levels in patients with cancer. **A,** Schematics of the FMD regimen, with the calorie content of each day of FMD (d1–d5). Black arrows indicate time points of blood/urine sample collection. Blood samples collected before the initiation of the FMD are indicated as "Pre," whereas samples collected after the end of five-day FMD (i.e., before the initiation of refeeding) are indicated as "Post." **B,** Bar plots indicating the number of patients (*y*-axis) who completed the number of FMD cycles indicated on the *x*-axis. **C,** Concentration of plasma glucose (mg/dL), serum insulin (10*µUI/mL), serum IGF1 (ng/mL), and urinary ketone bodies (mg/dL) before (Pre) and after (Post) FMD (first cycle) in 99 patients with cancer. **D,** Plasma glucose concentration (mg/dL) before and after FMD (across eight cycles; C1–C8). **E,** Serum insulin concentration (µUI/mL) before and after FMD (across eight cycles; C1–C8). **F,** Serum IGF1 concentration (ng/mL) before and after FMD (across eight cycles; C1–C8). **G,** BMI before and after FMD cycles (C1–C8) in the whole patient population. **H,** BMI before and after FMD (C1–C8) in patients undergoing FMD and cytotoxic chemotherapy (ChT). **I,** BMI before and after FMD (C1–C8) in patients undergoing FMD in combination with treatment other than ChT. All *P* values were determined by paired Wilcoxon test: *, $P < 0.05$; **, $P < 0.01$; ***, $P < 0.001$; ****, $P < 0.0001$. All comparisons for which the *P* value is not indicated did not show statistically significant differences ($P \geq 0.05$). Data are represented as box plots showing median values, with the boundaries of the rectangle representing the first and third quartiles, while whiskers extend to the extreme data points that are no more than 1.5 times the interquartile range.

RESULTS

Cyclic FMD Is Safe in Combination with Standard Anticancer Treatments

After excluding 17 patients not fulfilling the enrollment criteria, 101 patients were enrolled in the NCT03340935 trial to undergo cyclic FMD (Supplementary Table S1) in combination with standard-of-care antitumor therapies, which were chosen before enrollment and independently of patient participation in the study (Supplementary Fig. S1; Fig. 1A; Table 1). An FMD cycle was defined as five-day FMD followed by 16 to 23 days of refeeding. Specifically, the duration of an FMD cycle was dependent on the schedule of concomitant antitumor treatment, and ranged between 21 and 28 days. Blood samples were collected before the initiation of each FMD cycle ("Pre") and at the end of five-day FMD ("Post") for blood cell counts and standard biochemical evaluations.

Overall, a total number of 440 FMD cycles were completed, with a median number of 4 FMD cycles. In detail, 100 (99%) patients completed at least one FMD cycle, 77 (76.2%) patients at least three FMD cycles, and 20 (19.8%) patients completed the maximum number of allowed FMD cycles ($n = 8$; Fig. 1B). Reasons for FMD discontinuation were: inability to maintain the body mass index (BMI) above 20 kg/m^2 (4%), poor acceptability of the FMD (10.9%), patient decision (14.9%), tumor progression (21.8%), adverse events (AE; 6.9%), completed treatment program (17.8%), or surgery (4%). With 23 minor and 6 major deviations, 72 (71.3%) patients were fully compliant with the FMD, while 95 (94.1%) patients were fully compliant or reported only minor deviations (Supplementary Table S2). Considering individual FMD cycles, the global compliance rate was 91.8% (404 of 440 cycles), with minor and major deviations reported in 29 (6.6%) and 7 (1.6%) FMD cycles, respectively.

The trial met its primary endpoint, with an incidence of severe grade 3 or 4 (G3/G4) FMD-related AEs of 12.9% (90% CIs: 7.8–19.7%), that is, significantly lower than the prespecified 20% threshold (Table 2). Overall, the most common AE was fatigue, which occurred in 90.2% of patients and was G3/G4 in 4% of patients. Other G3/G4 FMD-related AEs were hypoglycemia (5%), syncope (1%), nausea (1%), dizziness (1%), and

Table 1. Clinical characteristics of patients enrolled in the NCT03340935 trial

		Patient population N = 101	
Characteristics		N	%
Age (years)	≥60	28	27.7
	< 60	73	72.3
Sex	Male	28	27.7
	Female	73	72.3
ECOG PS	0	63	62.4
	1	38	37.6
Tumor type	Breast	56	55.4
	• Luminal	• 26	• 46.4
	• TNBC	• 19	• 33.9
	• HER2+	• 11	• 19.7
	Colorectal	10	9.9
	• *KRAS* mutated	• 4	• 40
	• *BRAF* mutated	• 5	• 50
	Lung	7	6.9
	Prostate	4	3.9
	Pancreas	3	3
	Melanoma	3	3
	Germinal	3	3
	Ovary	2	2
	Thyroid	2	2
	Chronic lymphocytic leukemia	2	2
	Non-Hodgkin lymphoma	2	2
	Uterus	1	1
	Sarcoma	1	1
	Multiple myeloma	1	1
	Stomach	1	1
	Kidney	1	1
	Mesothelioma	1	1
	Myelofibrosis	1	1
Disease stage	Advanced	75	74.3
	Localized	26	25.7
Concomitant treatment	Chemotherapy	73	72.3
	Endocrine (± targeted therapies)	13	12.9
	Immunotherapy	3	2.9
	Targeted therapy	2	2
	Radiotherapy	1	1
	Radionuclide treatment	1	1
	Best supportive care	8	7.9
BMI at enrollment	20–24.9 kg/m^2	53	52.5
	25–29.9 kg/m^2	32	31.7
	30–34.9 kg/m^2	14	13.9
	>35 kg/m^2	2	1.9

increased aspartate aminotransferase levels (1%). Of note, only one (1%) G4 AE was reported (hypoglycemia), while serious AEs (SAE) occurred in 4 patients (4.0%), and in 2 of these cases they were attributable to the FMD (syncope, severe fatigue).

The FMD Favorably Modulates Key Blood Metabolic Parameters

In 99 evaluable patients the FMD reduced median plasma glucose concentration by 18.6% (range: −63.1%; +67.8%), serum insulin by 50.7% (range: −91.3%; +697%), and serum IGF1 by 30.3% (range: −72.3%; +139.8%), while it increased average urinary ketones from 0.18 mg/dL to 59.9 mg/dL (Fig. 1C). Of note, FMD-induced metabolic changes were independent of the type of primary tumor (breast cancer, colorectal cancer, lung cancer, others), concomitant anticancer treatments (ChT, other therapies) and tumor stage (limited, advanced; Supplementary Fig. S2A–S2C). Similar metabolic modifications occurred in 9 healthy volunteers undergoing the same five-day FMD regimen

Table 2. FMD-related AEs

AEs	G1 *n* (%)	G2 *n* (%)	G3 *n* (%)	G4 *n* (%)
Clinical symptoms				
Fatigue	33 (32.7)	54 (53.5)	4 (4.0)	0
Headache	39 (38.6)	1 (1.0)	0	0
Insomnia	14 (13.9)	2 (2.0)	0	0
Somnolence	5 (5.0)	1 (1.0)	0	0
Constipation	9 (8.9)	0	0	0
Muscle cramps	14 (13.9)	4 (4.0)	0	0
Dizziness	28 (27.7)	8 (7.9)	1 (1.0)	0
Nausea	34 (33.7)	14 (13.9)	1 (1.0)	0
Vomiting	18 (17.8)	3 (3.0)	0	0
Syncope	0	0	1 (1.0)	0
Presyncope	5 (5.0)	2 (2.0)	0	0
Tachycardia	5 (5.0)	2 (2.0)	0	0
Epigastric pain	9 (8.9)	4 (4.0)	0	0
Hot flushes	6 (5.9)	0	0	0
Chills	4 (4.0)	0	0	0
Tremor	3 (3.0)	1 (1.0)	0	0
Weight loss	77 (76.2)	0	0	0
Blood test alterations				
Hypoglycemia	25 (24.8)	17 (16.8)	4 (4.0)	1 (1.0)
AST increased	28 (27.7)	0	1 (1.0)	0
ALT increased	27 (26.7)	2 (2.0)	0	0
Uricemia increased	13 (12.9)	0	0	0
Total cholesterol increased	18 (17.8)	1 (1.0)	0	0
Hypertriglyceridemia	13 (12.9)	2 (2.0)	0	0
Creatinine increased	5 (5.0)	0	0	0
Total FMD-related adverse events	100 (99.0)	70 (69.3)	12 (11.9)	1 (1.0)

NOTE: Total rate of G3/4 FMD-related adverse events: 12.9%; 90% confidence interval: 7.8–19.7.

Abbreviations: ALT, alanine aminotransferase; AST, aspartate aminotransferase; G, grade.

(Supplementary Fig. S3A), but not in a cohort of 13 patients with advanced breast cancer enrolled in an observational study (INT 79/17; Supplementary Table S3) and treated with standard ChT without the FMD (Supplementary Fig. S3B).

During eight subsequent cycles, the FMD resulted in qualitatively and quantitatively similar modifications of key metabolic parameters, with a consistent reduction of plasma glucose, serum insulin, and IGF1 concentration (Fig. 1D–F), thus excluding the occurrence of systemic metabolic adaptation to the FMD. Each FMD cycle also reduced patient BMI (first cycle: median reduction: 4.52%; second cycle: median reduction: 4.51%; third cycle: median reduction: 4.55%) regardless of concomitant treatments (Fig. 1G–I). During the first three FMD cycles, the BMI was only partially recovered, thus resulting in progressive BMI reduction (Fig. 1G). Of note, this occurred only in patients receiving concomitant ChT, and was reversed after three FMD cycles (Fig. 1G and H).

Cyclic FMD Downregulates Peripheral Blood Immunosuppressive Myeloid Cells While Boosting Activated/Cytotoxic Cells

In 38 patients, we used multicolor flow cytometry to investigate the impact of the FMD on the frequency of myeloid and lymphocytic peripheral blood mononuclear cell (PBMC) populations (Supplementary Table S4; Supplementary Fig. S4A–S4C and S4E–S4G). At the end of five-day FMD, we found a significant decrease of total monocytes ($CD14^+$) and of two highly immunosuppressive monocyte subsets, that is, those lacking HLA-DR expression ($CD14^+HLA\text{-}DR^-$), acknowledged as monocytic myeloid-derived suppressor cells (M-MDSC; refs. 8, 9), and $CD14^+$ cells expressing PD-L1 ($CD14^+PD\text{-}L1^+$; ref. 10; Fig. 2A). The FMD also reduced low-density $CD15^+$ granulocytes, which include polymorphonuclear MDSCs (PMN-MDSC; Fig. 2A). Interestingly, the observed modifications in myeloid subpopulations were similar in patients undergoing the FMD in combination with ChT or with other standard antitumor therapies (Supplementary Fig. S5A and S5B).

To evaluate FMD-induced immunologic changes in a more homogeneous patient cohort, among these 38 patients, we selected a subset of 13 patients with advanced triple-negative breast cancer (TNBC) treated with first-line ChT–FMD combination (Supplementary Table S5), and we compared their PBMC profiles before and after FMD with immunologic modifications occurring in a matched cohort of 13 patients with advanced breast cancer treated with first-line ChT without the FMD (Supplementary Table S3). Notably, $CD14^+HLA\text{-}DR^-$, $CD14^+PD\text{-}L1^+$

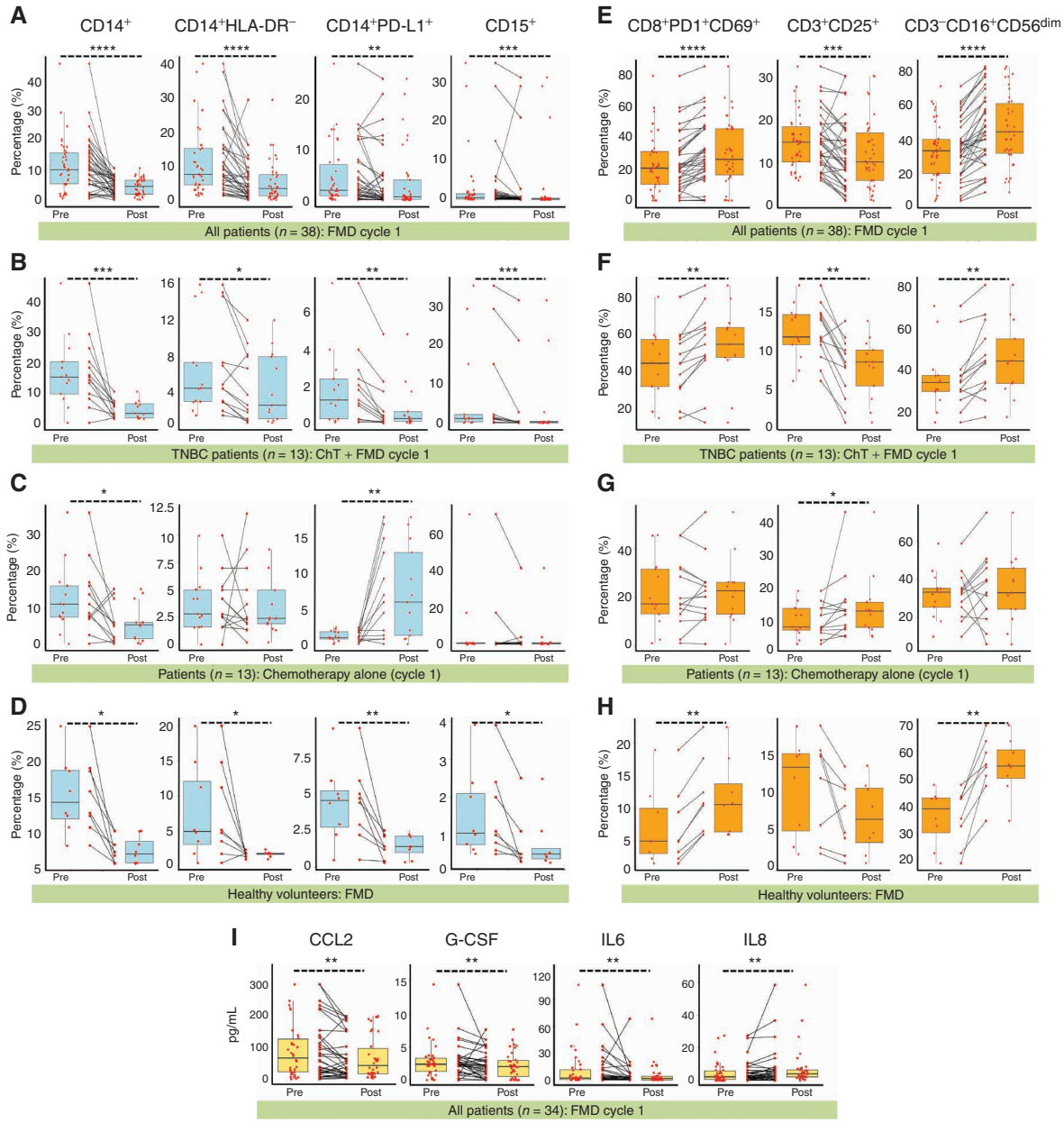

Figure 2. The fasting-mimicking diet (FMD) reduces peripheral blood immunosuppressive cells and increases effector cells in patients with cancer and in healthy volunteers. **A,** Frequencies of CD14+, CD14+HLA-DR−, CD14+PD-L1+, and CD15+ cells before (Pre) and after (Post) FMD (first cycle) in 38 patients with different tumor types enrolled in the NCT03340935 trial. CD14+ and CD15+ cells were calculated as frequencies in total PBMCs (after debris and doublet exclusion), while CD14+PD-L1+ and CD14+HLA-DR− cells were calculated as frequencies in total CD14+ cells. **B,** Frequencies of CD14+, CD14+HLA-DR−, CD14+PD-L1+, and CD15+ cells before (Pre) and after (Post) FMD (first cycle) in 13 patients with advanced breast cancer enrolled in the NCT03340935 trial and treated with first-line ChT plus FMD. **C,** Frequencies of CD14+, CD14+HLA-DR−, CD14+PD-L1+ and CD15+ cells before (Pre) and after (Post) ChT in a cohort of 13 patients with advanced breast cancer treated with ChT without the FMD. **D,** Frequencies of CD14+, CD14+HLA-DR−, CD14+PD-L1+, and CD15+ cells before (Pre) and after (Post) FMD in 8 healthy volunteers. **E,** Frequencies of pre- and post-FMD CD8+PD1+CD69+ (among CD3+CD69+), CD3+CD25+ (among CD3+), and CD3−CD16+CD56dim (among CD3−) cells in 38 patients with different tumor types enrolled in the NCT03340935 trial. **F,** Frequencies of pre- and post-FMD CD8+PD1+CD69+ (among CD3+CD69+), CD3+CD25+ (among CD3+) and CD3−CD16+CD56dim (among CD3−) cells in 13 patients with advanced breast cancer enrolled in the NCT03340935 trial and treated with first-line ChT plus FMD. **G,** Frequencies of CD8+PD-1+CD69+ (among CD3+CD69+), CD3+CD25+ (among CD3+), and CD3−CD16+CD56dim (among CD3−) cells before and after ChT in 13 patients with advanced breast cancer treated with ChT without the FMD. **H,** Frequencies of pre- and post-FMD CD8+PD-1+CD69+ (among CD3+CD69+), CD3+CD25+ (among CD3+), and CD3−CD16+CD56dim (among CD3−) cells in 8 healthy volunteers. **I,** Plasma concentration of CCL2, G-CSF, IL6, and IL8, as evaluated at the initiation and at the end of the FMD, in 34 patients with different tumor types enrolled in the NCT03340935 trial. CCL2, C-C motif chemokine ligand 2. All *P* values were determined by paired Wilcoxon test: *, $P < 0.05$; **, $P < 0.01$; ***, $P < 0.001$; ****, $P < 0.0001$. All comparisons for which the *P* value is not indicated did not show statistically significant differences ($P \geq 0.05$). Box plots indicate median values of the indicated variable, with the boundaries of the rectangle representing the first and third quartiles, while vertical black lines extend to the extreme data points that are no more than 1.5 times the interquartile range. Each red dot represents one patient; couples of dots connected by the same black line refer to data from the same patient before and after the FMD.

and CD15$^+$ cells were downmodulated in patients receiving the ChT–FMD combination (Fig. 2B), but not in patients treated with ChT alone, which even resulted in a boost of CD14$^+$PD-L1$^+$ cells (Fig. 2C). Finally, in 8 healthy volunteers, the FMD reduced CD14$^+$, CD14$^+$HLA-DR$^-$, CD14$^+$PD-L1$^+$, and CD15$^+$ cells similarly to what was observed in patients with cancer (Fig. 2D).

FMD-induced reduction of myeloid cell subsets was paralleled by an increase of activated CD8$^+$ T cells (coexpressing PD-1 and CD69) and cytolytic CD3$^-$CD16$^+$CD56^{dim} natural killer (NK) cells (11), while CD3$^+$ T cells expressing the high-affinity IL2 receptor (CD3$^+$CD25$^+$ cells), which can be associated with Treg activity, were reduced (Fig. 2E). As in the case of myeloid cells, changes in lymphocytic populations occurred independently of concomitant antitumor therapies (Supplementary Fig. S5C and S5D), and they were confirmed in a homogeneous subset of 13 patients with TNBC treated with first-line ChT plus FMD (Fig. 2F), but not in 13 patients with breast cancer treated with ChT alone (Fig. 2G). Interestingly, the FMD increased CD8$^+$PD-1$^+$CD69$^+$ and CD3$^-$CD16$^+$CD56^{dim} cells in 8 healthy volunteers in a similar way as observed in patients (Fig. 2H).

Because PD-1 is a marker shared by activated and exhausted CD8$^+$ T cells, in 12 patients undergoing the FMD without concomitant ChT (to avoid confounding effects), we performed a deeper immune profiling to gain insight into the functional properties of CD8$^+$ T cells and other relevant T-cell subsets (Supplementary Fig. S4C–S4F). Notably, CD8$^+$PD-1$^+$ T cells collected after the FMD displayed remarkably increased expression of activation markers, such as Granzyme B (but not Ki-67; Supplementary Fig. S5E) and IFNγ upon T-cell receptor triggering (Supplementary Fig. S5F), while CD8$^+$PD-1$^+$ T cells not expressing the immune checkpoints LAG3 and TIM3 were increased, thus excluding their exhaustion (Supplementary Fig. S5G). In addition, we observed an enrichment of CD3$^+$CCR7$^-$CD45RA$^-$ cells within CD3$^+$ T lymphocytes (Supplementary Fig. S5H), which suggests the acquisition of an effector-memory phenotype (12). Finally, Tregs (CD4$^+$CD127$^-$CD25^{hi}FOXP3$^+$ cells) were reduced after the FMD (Supplementary Fig. S5I), possibly explaining the decrease of CD3$^+$CD25$^+$ cells (Fig. 2E).

During the second FMD cycle, myeloid and lymphoid PBMC populations were modulated in a similar way as during the first FMD cycle (Supplementary Fig. S5J and S5K), thus excluding the adaptation to FMD-induced systemic immunologic effects.

To gain insight into potential mechanisms explaining the observed modulation of peripheral blood immune cell populations, we measured blood cytokines/chemokines associated with myeloid and lymphoid mobilization and/or activation in plasma samples collected before and after the FMD in 34 of these patients. As shown in Supplementary Fig. S6, most of these molecules were not detectable in the majority of patients, or they did not undergo significant changes during the FMD. However, CCL2, G-CSF, and IL6, which are involved in myeloid cell mobilization from the bone marrow, were significantly reduced after the FMD, while we found a modest increase of IL8 levels (Fig. 2I).

Together, these data indicate that the FMD, alone or in combination with standard antitumor therapies, downregulates immunosuppressive myeloid cell subsets, while at the same time increasing effector cells with an activated phenotype. In contrast, ChT alone does not affect most of these cell subsets, and it can even boost highly immunosuppressive CD14$^+$PD-L1$^+$ cells.

The FMD Reshapes Intratumor Immunity in Patients with Breast Cancer

To investigate whether the FMD modulates intratumor immunity, we performed an unplanned, interim analysis of the ongoing DigesT trial (NCT03454282), a window-of-opportunity study in which patients with early-stage breast cancer or melanoma undergo five-day FMD followed by surgery after 7 to 10 days (see Methods for details). To this aim, we selected 22 patients with consecutive breast cancer participating in the trial, and for whom a sufficient amount of formalin-fixed, paraffin-embedded (FFPE) tumor material collected before the FMD (tumor biopsies) and after the FMD (surgical specimens) was available to perform IHC and RNA-sequencing (RNA-seq) analyses for the evaluation of tumor-infiltrating immune cells and transcriptomic immune profiles (Supplementary Fig. S7; Supplementary Table S6; Fig. 3A).

Figure 3. The fasting-mimicking diet (FMD) reshapes intratumor immunity in patients with breast cancer. **A,** Time points of blood and tissue sample collection in the DigesT trial (NCT03454282). T1, initiation of the FMD; T2, end of the FMD; T3, surgery; T4, approximately 30 days after surgery. **B,** Left, IHC evaluation of intratumor IGFR1 and phosphorylated IGFR1 (pIGF1R; brown dots) in pre- and post-FMD tumor samples from one indicative patient (magnification of 200×). **B,** Right, Box plots showing results of IHC analyses (reported as H-score) of IGF1R and pIGF1R in matched pre- and post-FMD tumor samples in 18 patients enrolled in the DigesT trial (NCT03454282). All *P* values for the indicated comparisons were determined by paired Wilcoxon test: *, $P < 0.05$; **, $P < 0.01$; ***, $P < 0.001$; ****, $P < 0.0001$. Box plots indicate median values, with the boundaries of the rectangle representing the first and third quartiles, while vertical black lines extend to the extreme data points that are no more than 1.5 times the interquartile range. Each red dot represents one patient; couples of plots connected by the same black line refer to the same patient before and after the FMD. **C,** Representative images of hematoxylin and eosin staining (H&E) and IHC evaluations of intratumor CD8$^+$ T cells and CD68$^+$ macrophages in pre-FMD (T1) and post-FMD (T3) tumor samples from two representative patients (magnification of ×200). **D**, Top plots, box plots showing the IHC quantification of percentage (area) and absolute average numbers (per high-power field; HPF) of intratumor stromal CD8$^+$ cells, absolute average number (per HPF) of intraepithelial CD8$^+$ cells, absolute average number (per HPF) of CD68$^+$ macrophages, and the ratio between stromal CD8$^+$ cells (absolute average number per HPF) and CD68$^+$ macrophages (absolute average number per HPF) in pre-FMD versus post-FMD tumor specimens. Box plot showing the *CD8A*/*CD68* transcript ratio in post-FMD as compared with pre-FMD tumor specimens. Box plots indicate median values of the frequencies of each immune cell population/gene transcript, with the boundaries of the rectangle representing the first and third quartiles, while vertical black lines extend to the extreme data points that are no more than 1.5 times the interquartile range. Each red dot represents one patient; couples of dots connected by the same black line refer to data from the same patient pre- and post-FMD. *, $P < 0.05$; **, $P < 0.01$; ***, $P < 0.001$ by paired Wilcoxon test for the indicated comparisons. **D,** Bottom plots, correlation between CD8$^+$ T cells by IHC and *CD8A* gene expression, and between CD68$^+$ macrophages by IHC and *CD68* gene expression; box plot showing the *CD8A*/*CD68* transcript ratio in post-FMD as compared with pre-FMD tumor specimens. **E,** Heat map displaying scores of enrichment of leukocyte subsets (XCell, Charoentong list) that are differentially modulated after the FMD [T3 vs. T1, paired Wilcoxon test, $P < 0.05$, Benjamini–Hochberg (B-H) false discovery rate (FDR) < 0.1]. aDC, activated DCs; CD4$^+$ and CD8$^+$ Tcm: CD4$^+$ and CD8$^+$ central memory T lymphocytes; NKT, natural killer T cells; pDC, plasmacytoid dendritic cells; Tem, effector memory T lymphocytes. **F,** Box plots representing scores of individual leukocyte subsets modulated in post-FMD versus pre-FMD tumor specimens. **G,** Matrix correlation displaying Spearman correlation coefficients between RNA-seq data (*CD8A* and *CD68* transcripts, CD8$^+$ T-cell, and Macrophage enrichment scores), and IHC assessment of CD8$^+$ T cells and CD68$^+$ cells.

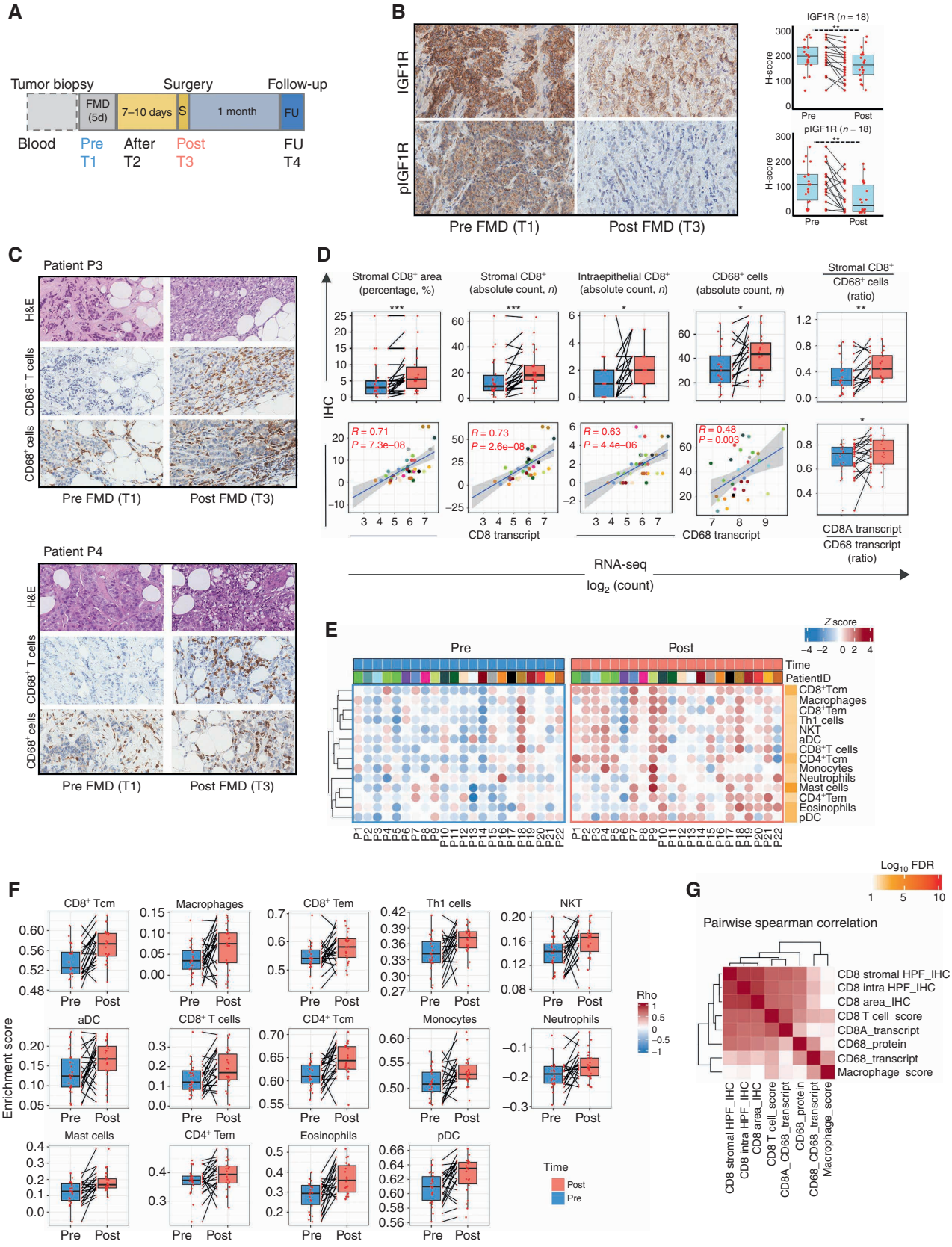
A
Tumor biopsy
Surgery
Follow-up
FMD (5d)
7–10 days
S
1 month
FU
Blood
Pre T1
After T2
Post T3
FU T4
B
IGF1R
pIGF1R
Pre FMD (T1)
Post FMD (T3)
IGF1R (n = 18)
pIGF1R (n = 18)
H-score
Pre
Post
C
Patient P3
Patient P4
H&E
CD68+ T cells
CD68+ cells
Pre FMD (T1)
Post FMD (T3)
D
Stromal CD8+ area (percentage, %)
Stromal CD8+ (absolute count, n)
Intraepithelial CD8+ (absolute count, n)
CD68+ cells (absolute count, n)
Stromal CD8+ / CD68+ cells (ratio)
IHC
R = 0.71
P = 7.3e−08
R = 0.73
P = 2.6e−08
R = 0.63
P = 4.4e−06
R = 0.48
P = 0.003
CD8 transcript
CD68 transcript
CD8A transcript / CD68 transcript (ratio)
RNA-seq
log2 (count)
E
Z score
Pre
Post
Time
PatientID
CD8+Tcm
Macrophages
CD8+Tem
Th1 cells
NKT
aDC
CD8+T cells
CD4+Tcm
Monocytes
Neutrophils
Mast cells
CD4+Tem
Eosinophils
pDC
F
CD8+ Tcm
Macrophages
CD8+ Tem
Th1 cells
NKT
aDC
CD8+ T cells
CD4+ Tcm
Monocytes
Neutrophils
Mast cells
CD4+ Tem
Eosinophils
pDC
Enrichment score
Rho
Time
Post
Pre
G
Log10 FDR
Pairwise spearman correlation
CD8 stromal HPF_IHC
CD8 intra HPF_IHC
CD8 area_IHC
CD8 T cell_score
CD8A_transcript
CD68_protein
CD68_transcript
Macrophage_score

In this patient cohort, we first confirmed that the FMD reduces blood glucose, insulin, and IGF1 concentration and increases urinary ketone bodies (Supplementary Fig. S8), thus recapitulating data from the NCT03340935 trial (Fig. 1C). Because of the biological relevance of blood IGF1 reduction in mediating fasting/FMD-induced antitumor effects in preclinical models (5, 6), we investigated if the observed reduction of blood IGF1 concentration affects IGF1 receptor (IGF1R) expression/activation at the tumor level. To this aim, we assessed by IHC analysis the expression of total IGF1R and phosphorylated (i.e., activated) IGF1R in 18 paired tumor specimens. Notably, we found a significant reduction in total and phosphorylated IGF1R in post-FMD surgical tumor specimens when compared with pre-FMD tumor biopsies (Fig. 3B), thus indicating that FMD-induced growth factor changes in the blood are reflected by consistent modifications of the corresponding biological pathways at the tumor level.

To assess the impact of the FMD on intratumor immunity, we evaluated tumor-infiltrating $CD8^+$ T cells, $CD68^+$ macrophages, and other immune cell subsets. IHC analysis revealed a statistically significant increment of tumor-infiltrating $CD8^+$ T cells in post-FMD surgical tumor samples when compared with pre-FMD tumor biopsies (Supplementary Table S7; Fig. 3C and D). *CD8A* gene expression was increased in post-FMD samples as well, and we found a strong, positive correlation between CD8 protein (IHC) and *CD8A* gene (mRNA) expression levels (Fig. 3D). While tumor-infiltrating macrophages ($CD68^+$ cells) were also upregulated after the FMD (Fig. 3C and D), the CD8/CD68 (protein) and *CD8A/CD68* (gene transcript) ratios, which were previously associated with better prognosis in patients with cancer (13), were increased in post-FMD tumor specimens (Fig. 3D).

To broadly evaluate the impact of the FMD on several tumor-infiltrating immune cell populations, we performed cell-type enrichment analysis of RNA-seq data according to a set of pan-cancer metagenes for 28 immune cell subpopulations (14). Notably, the FMD increased total $CD8^+$ T cells and $CD8^+$ T cells with Th1 polarization, along with other immune cell populations potentially implicated in antitumor immune response, such as NKT, activated dendritic cells (aDC), and central and effector memory $CD4^+$ and $CD8^+$ T cells ($CD4^+$ Tcm, $CD4^+$ Tem, $CD8^+$ Tcm, $CD8^+$ Tem; Fig. 3E and F; Supplementary Tables S8 and S9). Estimates of intratumor $CD8^+$ T cells positively correlated with IHC scores of CD8 and with *CD8A* gene expression levels, thus confirming the reliability of cell-type enrichment analysis (Fig. 3G). Finally, when macrophages were stratified into M1-like and M2-like subtypes (15), we detected an increase of M1-like macrophages after the FMD, while M2-like macrophages did not significantly change (Supplementary Fig. S9A). Together, these results indicate a switch of the functional orientation of the tumor microenvironment toward a favorable/cytotoxic Th1/M1-like phenotype.

The FMD Activates Convergent Intratumor Immune Programs Leading to Relieved Immune Suppression and Enhanced T-cell Activation

To investigate the functional relevance of FMD-induced changes in tumor-infiltrating immune cell populations, we evaluated by RNA-seq analysis the modulation of immune transcriptomic signatures with prognostic/predictive relevance, or associated with the functional status of tumor-infiltrating immune cells (Supplementary Table S10). Overall, the FMD induced profound changes of intratumor transcriptional programs (Supplementary Tables S11–S13). Single-gene level analysis revealed a dramatic increase in the expression of several immune-related genes (see Methods for details; Fig. 4A). Notably, the IFNγ-activating signature (IFNG.GS), which is selectively activated in tumor-infiltrating immune cells and is associated with favorable clinical outcomes (16), was enriched in post-FMD tumor specimens, while the IFNγ-resistant signature (ISG.RS), which is prevalently expressed in cancer cells and is associated with resistance to immunotherapy through the induction of T-cell exhaustion, was not significantly modulated (Fig. 4A and B). Moreover, all the top upregulated immune genes in post-FMD tumor specimens belonged to the IFNG.GS signature (Fig. 4A and B).

Consistent with these data, the FMD induced an enrichment of 13 immune-related gene expression signatures (including IFNG.GS) previously associated with favorable prognosis in patients with cancer, including patients with breast cancer (see Methods; Supplementary Tables S12 and S13). Among them, 12 had at least one transcript passing the FDR cutoff of 0.1 (Fig. 4B, top, and C). In addition, among a list of exhaustion, costimulatory, and inhibitory markers (immune checkpoints; see Methods and Supplementary Table S10), the only transcripts significantly upregulated by the FMD were *CTLA4* and *LGALS9*, consistent with T-cell activation and cytotoxicity, as suggested by the upregulation

Figure 4. Intratumor transcriptomic changes induced by fasting-mimicking diet (FMD). **A,** Volcano plots displaying differentially expressed genes comparing post-FMD (T3) versus pre-FMD (T1) gene-level RNA-seq data using negative binomial distribution (Deseq2 package). Benjamini–Hochberg (B-H) false discovery rate (FDR) and Log_2 fold change are represented. Left, red and blue colors are used to display upregulated and downregulated transcripts in post-FMD versus pre-FMD tumors, respectively; immune-related genes (see Methods and Supplementary Table S10) are colored in dark red (upregulated in post-FMD versus pre-FMD comparison) and dark blue (downregulated in post-FMD versus pre-FMD comparison); all the immune-related genes with $-\log_{10}$ FDR > 2.5 are labeled; additional representative immune-related genes with $-\log_{10}$ FDR > 1 are labeled; in the middle and left panels, transcripts belonging to the IFN-activating signature (IFNG.GS) and IFN-resistant signature (ISG.RS) are colored in purple and green, respectively. Volcano plot *y*-axis is truncated at $-\log_{10}$ FDR = 10, as no immune-related genes above that cutoff were present. **B,** Heat maps representing differentially expressed genes in post-FMD (T3, surgical samples) versus pre-FMD (T1, tumor biopsies) comparisons; the top panel displays genes with $P < 0.05$ (Wilcoxon test) and B-H FDR < 0.1 at differential gene expression analysis and included in any of the significantly modulated ($P < 0.05$ and B-H FDR < 0.1) prognostic/predictive signatures at single-sample gene set enrichment analysis (of the 25 evaluated prognostic/predictive signatures, 13 were significantly enriched in post-FMD vs. pre-FMD tumor samples, but one of them did not yield any differentially expressed genes, therefore only 12 signatures are represented in the heat map; Supplementary Table S10); the middle panel displays genes with $P < 0.05$ (Wilcoxon test) and B-H FDR < 0.1 at differential gene expression analysis and included in the exhaustion and immune checkpoint list (Supplementary Table S10); the bottom panel displays genes with $P < 0.05$ and B-H FDR < 0.1 at differential gene expression analysis and included in the cytokine/chemokine gene list (Supplementary Table S10). In the heat maps, all genes with B-H FDR < 0.05 are labeled, in addition with other selected genes (in brackets) with FDR between 0.1 and 0.05. **C,** Box plots of representative prognostic/predictive signature enrichment scores and transcripts with $P < 0.05$ and B-H FDR < 0.1 in the post-FMD (T3) versus pre-FMD (T1) comparison. **D,** Box plots of Perforin 1 and Granzyme B IHC scores in post-FMD (T3) versus pre-FMD (T1) tumors ($n = 17$ and $n = 16$, respectively).

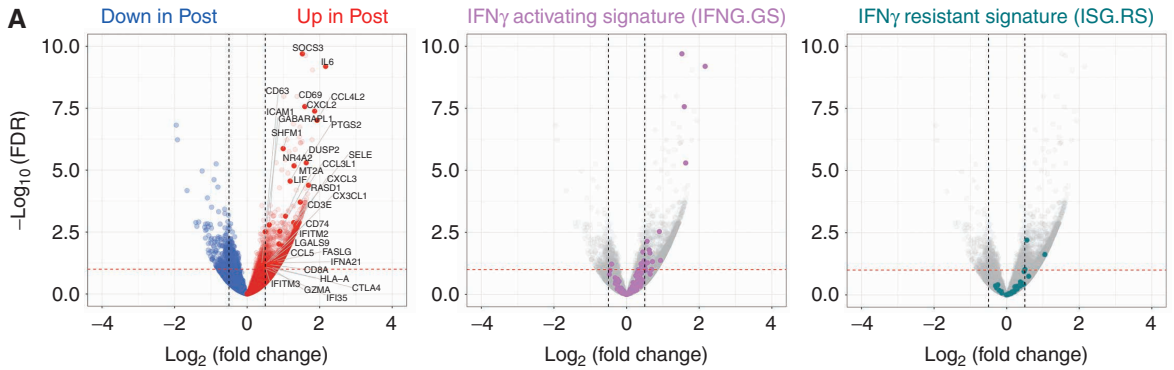
A
Down in Post
Up in Post
IFNγ activating signature (IFNG.GS)
IFNγ resistant signature (ISG.RS)
−Log10 (FDR)
Log2 (fold change)

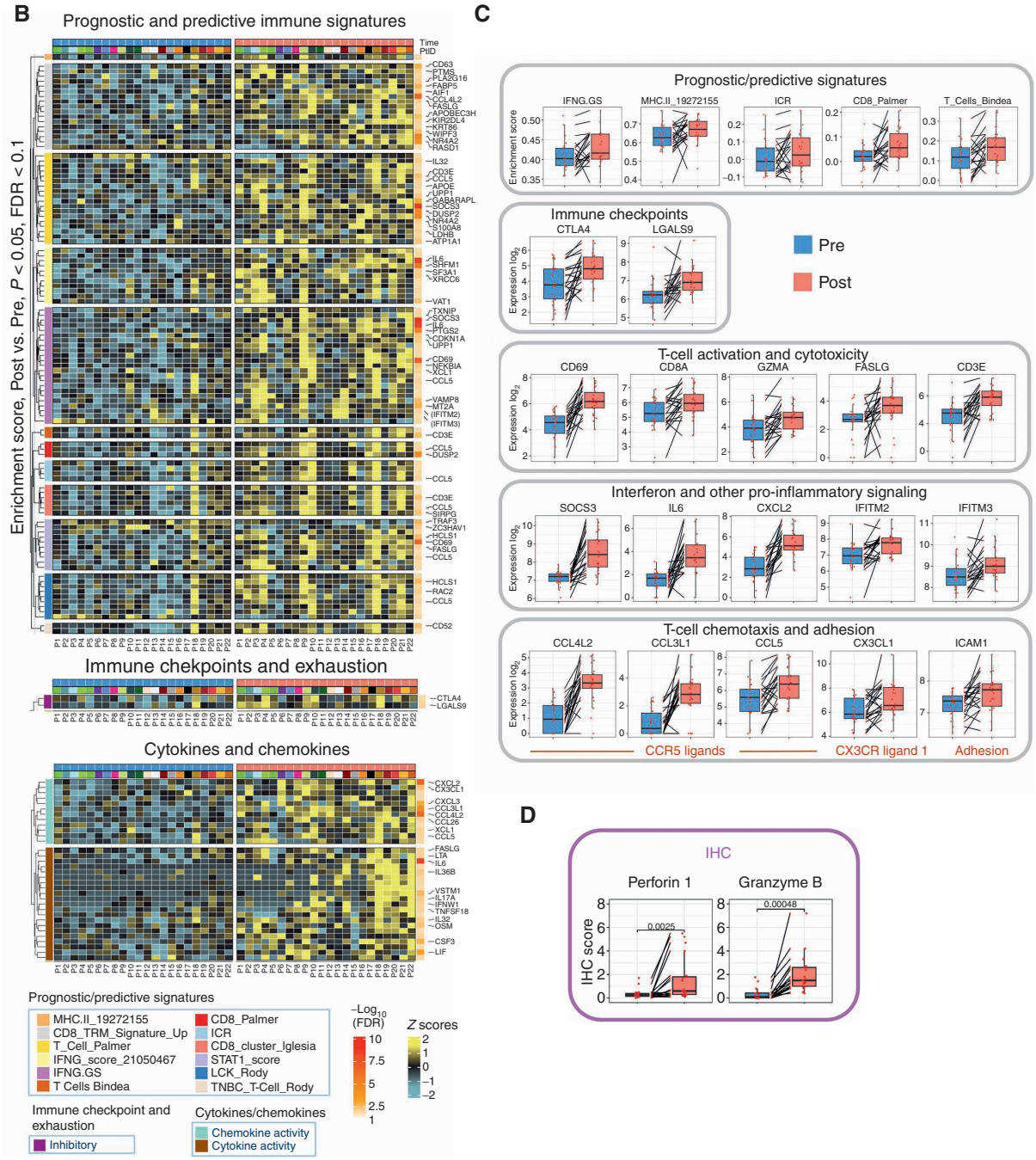
B
Prognostic and predictive immune signatures
Enrichment score, Post vs. Pre, P < 0.05, FDR < 0.1
Immune chekpoints and exhaustion
Cytokines and chemokines
Prognostic/predictive signatures
MHC.II_19272155
CD8_Palmer
CD8_TRM_Signature_Up
ICR
T_Cell_Palmer
CD8_cluster_Iglesia
IFNG_score_21050467
STAT1_score
IFNG.GS
LCK_Rody
T Cells Bindea
TNBC_T-Cell_Rody
Immune checkpoint and exhaustion
Inhibitory
Cytokines/chemokines
Chemokine activity
Cytokine activity
C
Prognostic/predictive signatures
IFNG.GS
MHC.II_19272155
ICR
CD8_Palmer
T_Cells_Bindea
Enrichment score
Immune checkpoints
CTLA4
LGALS9
Expression log2
Pre
Post
T-cell activation and cytotoxicity
CD69
CD8A
GZMA
FASLG
CD3E
Interferon and other pro-inflammatory signaling
SOCS3
IL6
CXCL2
IFITM2
IFITM3
T-cell chemotaxis and adhesion
CCL4L2
CCL3L1
CCL5
CX3CL1
ICAM1
CCR5 ligands
CX3CR ligand 1
Adhesion
D
IHC
Perforin 1
Granzyme B
IHC score
0.0025
0.00048

of *CD69*, *CD8A*, *GZMA*, *FASLG*, and *CD3E* genes (Fig. 4B and C), and confirmed by an increased IHC expression of Perforin 1 and Granzyme B expression (Supplementary Fig. S9B; Fig. 4D). In line with these data, several markers associated with IFN or other proinflammatory signaling axes (such as *SOCS3*, *IL6*, *CXCL2*, *IFITM2*, and *IFITM3*, which are also part of the IFNG.GS signature) were upregulated after the FMD (Fig. 4B and C). This intense cytotoxic response can in part be explained by the recruitment of activated/cytotoxic T cells through the CCR5/CX3CR1 chemokine pathways, as suggested by the upregulation of genes encoding CCR5/CX3CR1 ligands (*CCL4L2*, *CCL3L1*, *CCL5*, and *CX3CL1*, respectively) and of the adhesion marker *ICAM1* (Fig. 4B and C), which are critical for immune-mediated tumor rejection. Finally, among Kyoto Encyclopedia of Genes and Genomes immune-related pathways that were found to be dysregulated by the FMD (see https://figshare.com/s/b0dd838c5a9f23847c7a and https://figshare.com/s/5da2261cfa3f0cc535d1), all of them were enriched in post-FMD tumor specimens, with the exception of the TGFβ pathway, which is often associated with immune suppression (Supplementary Fig. S10).

Together, these results show that five-day FMD is sufficiently potent to broadly reshape intratumor immunity within 7 to 10 days in patients with limited-stage breast cancer, thus reducing biomarkers associated with immune suppression and promoting tumor infiltration by activated and cytotoxic immune cell populations.

FMD-Induced Relief of Systemic Myeloid Immune Suppression Is Associated with Enhanced Intratumor T-cell Cytotoxicity

We next applied high-dimensional flow cytometry analysis to PBMCs from 19 of the 22 DigesT patients to deeply dissect the modulation of myeloid and lymphoid PBMC subsets at the end of the FMD (T2) and at subsequent time points (T3: surgery, occurring 7–10 days after the end of the FMD; T4: ~30 days after surgery; Fig. 5A). Immune cell subsets captured by this analysis and the gating strategy of the main populations are depicted in Supplementary Figs. S11A, S11B, S12, and S13. As summarized in the heat map in Fig. 5A, we observed a remarkable modulation of diverse immune cell subsets encompassing both myeloid and lymphoid populations. In particular, the FMD reduced total $CD14^+$ monocytes, M-MDSCs and PMN-MDSCs, including the PMN-MDSC subset expressing the lectin-type oxidized LDL receptor-1 ($LOX1^+$; ref. 17). In parallel, we observed a significant boost of classical monocytes expressing HLA-DR (CMo DR^+), which have been correlated with clinical benefit from immunotherapy in patients with melanoma (18), as well as of intermediate monocytes (IMo), which are associated with good prognosis in patients with breast cancer (19). Interestingly, circulating $CD14^+$ cells collected after the FMD showed reduced expression of CCL2 receptor (CD192) and fractalkine receptor (CX3CR1) prevalently in the HLA-DR^- subset, indicating a reduction of proinflammatory/immunosuppressive functions and chemokine-directed tumor trafficking. Finally, we observed an increment of DCs and $CD16^+$ DCs, the latter representing a unique myeloid antigen-presenting cell population with enhanced T-cell priming ability (20). The FMD also profoundly affected T cells, particularly the $CD8^+$ subset, with a remarkable upregulation of PD-1 and an enhancement of the effector phenotype, as suggested by the increment of CD28-negative ($CD28^-$) T cells and an increased expression of CX3CR1, which identifies a subset of antigen-experienced cells involved in immunosurveillance (21) and associated with clinical benefit from anti–PD-1 therapy (ref. 22; Fig. 5A). Several subsets of Tcm and Tem cells (e.g., TEMRA $CD8^+$ T cells, TCM $CD8^+$, TCM $CD8^+$ $PD1^+$) were also significantly increased after the FMD, which instead reduced exhausted and hyperexhausted ($PD\text{-}1^+LAG3^+TIM3^+$) T cells, Tregs, and $CD8^+CD25^+$ cells, possibly representing $CD8^+$ Tregs (Fig. 5A; ref. 23). Finally, the FMD globally boosted the NK compartment in both $CD56^{bright}$ and $CD56^{dim}$ subsets, as well as circulating B cells (Fig. 5A).

Notably, some FMD-induced immune modifications that occurred precociously (T2) were maintained at later time points, that is, at surgery (T3) and 1 month after surgery (T4; Fig. 5A and B). In particular, the downregulation of the myeloid compartment (including several monocytic and MDSC subsets) and the boost of NK cells were maintained throughout the observation time; by contrast, the FMD effect on several T-cell subsets tended to be mitigated at later time points (Fig. 5B). Regression plots of all the immune cell populations shown in the heat map of Fig. 5A, and not included in Fig. 5B, are depicted in Supplementary Fig. S14. Line plots indicating the kinetics of all immune populations reported in the heat map of Fig. 5A are depicted in Supplementary Fig. S15.

Then we correlated the immunomodulatory effects of the FMD in the blood and in the tumor at a single patient level and at the same time points (pre-FMD for tumor specimens and T1 for PBMCs; post-FMD for tumor specimens and T3 for PBMCs; see Fig. 5C and D and Supplementary Tables S14–S16). Overall, the contraction of peripheral blood myeloid-suppressive compartment was associated with an enhanced intratumor T-cell cytotoxicity (Fig. 5C). Of note, intratumor cytotoxic/memory $CD4^+$ T cells, $CD8^+$ T cells, and Th1 cells positively correlated with several peripheral blood activated/effector T-cell populations (e.g., TEM, TEM $PD\text{-}1^+$), and at the same time they negatively correlated with exhausted/hyperexhausted T cells (e.g., $CD8^+PD\text{-}1^+LAG3^+$,

Figure 5. Dynamic effects of FMD on systemic immunity and correlation with transcriptional immune modulation at tumor site. High-dimensional flow cytometry was performed in PBMCs from 19 of 22 patients enrolled in the DigesT trial selected for tumor RNA-seq analysis. **A,** Samples for high-dimensional flow cytometry were collected before the FMD (T1) and at different time points after the FMD (T2, T3, T4). We assessed the expression of multiple lymphoid and myeloid markers to define a total of 120 cell subsets (see Supplementary Fig. S11–S13). The nonparametric paired Wilcoxon test was used to compare the diverse immune cell frequencies at T2 versus T1, T3 versus T1, and T4 versus T1; 57 PBMC subpopulations undergoing modifications passing the significance cutoff at least at one time point ($P < 0.05$, Benjamini-Hochberg FDR < 0.1) are represented in the heat map. **B,** Loess regression curves of representative immune cell subsets are shown to illustrate modulation across time. See Supplementary Fig. S14 for the representation of the remaining PBMC Loess regression curves related to the significantly modulated PBMC subsets. **C,** Heat map representing Spearman correlations between significantly modulated blood PBMC subpopulations ($n = 57$) and intratumor leucocyte subsets ($n = 14$) at T3 versus T1 in 19 patients for whom both PBMC flow cytometry and tumor RNA-seq data were available. **D,** Representative correlations between individual patient values of the indicated PBMC and intratumor leukocyte subsets ($P < 0.05$, Benjamini–Hochberg FDR < 0.1) at T1 and T3.

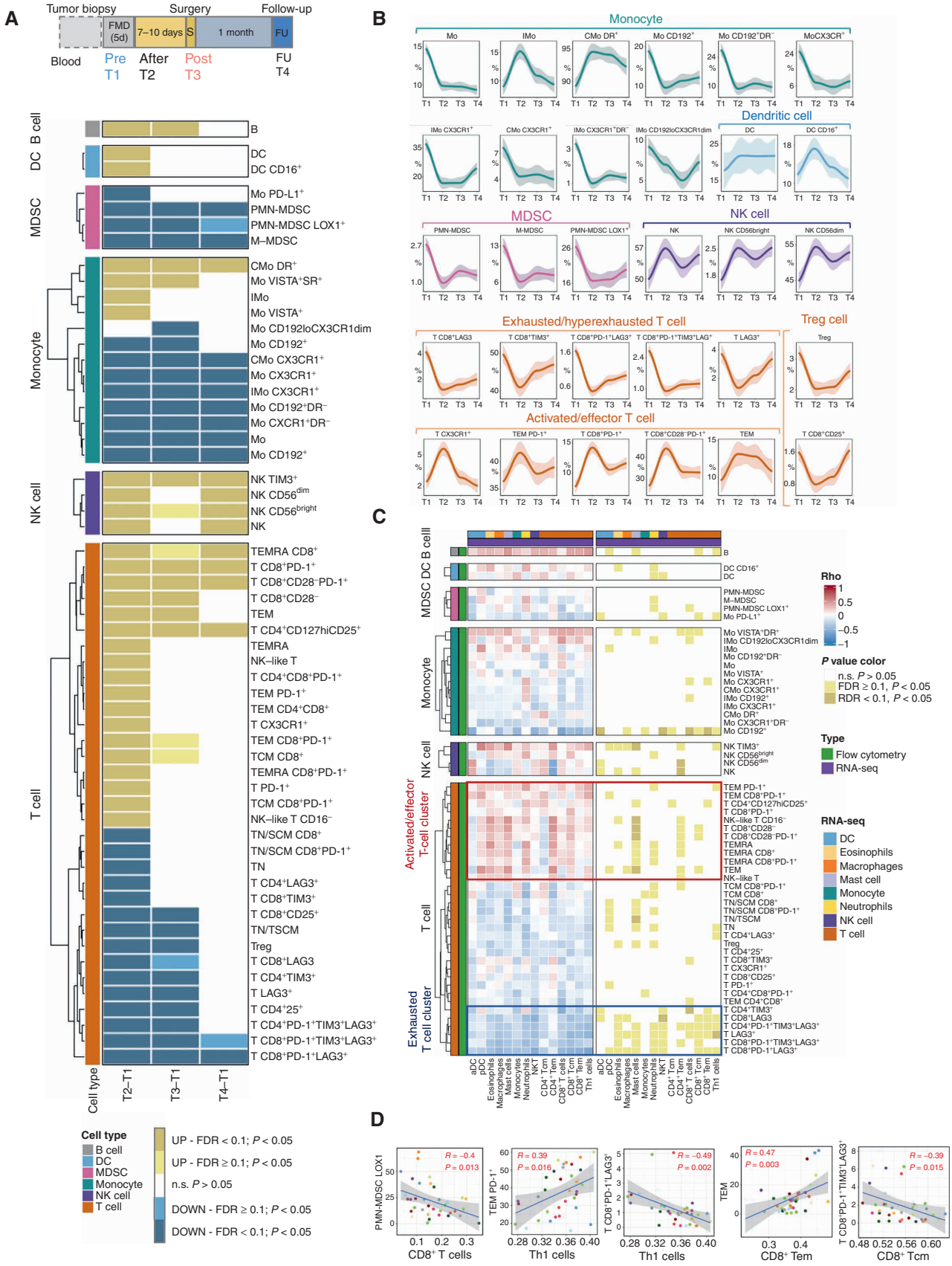
A
Tumor biopsy
Surgery
Follow-up
FMD (5d)
7–10 days
S
1 month
FU
Blood
Pre T1
After T2
Post T3
FU T4
B cell
DC
MDSC
Monocyte
NK cell
T cell
B
DC
DC CD16+
Mo PD-L1+
PMN-MDSC
PMN-MDSC LOX1+
M–MDSC
CMo DR+
Mo VISTA+SR+
IMo
Mo VISTA+
Mo CD192loCX3CR1dim
Mo CD192+
CMo CX3CR1+
Mo CX3CR1+
IMo CX3CR1+
Mo CD192+DR–
Mo CXCR1+DR–
Mo
Mo CD192+
NK TIM3+
NK CD56dim
NK CD56bright
NK
TEMRA CD8+
T CD8+PD-1+
T CD8+CD28–PD-1+
T CD8+CD28–
TEM
T CD4+CD127hiCD25+
TEMRA
NK–like T
T CD4+CD8+PD-1+
TEM PD-1+
TEM CD4+CD8+
T CX3CR1+
TEM CD8+PD-1+
TCM CD8+
TEMRA CD8+PD-1+
T PD-1+
TCM CD8+PD-1+
NK–like T CD16–
TN/SCM CD8+
TN/SCM CD8+PD-1+
TN
T CD4+LAG3+
T CD8+TIM3+
T CD8+CD25+
TN/TSCM
Treg
T CD8+LAG3
T CD4+TIM3+
T LAG3+
T CD4+25+
T CD4+PD-1+TIM3+LAG3+
T CD8+PD-1+TIM3+LAG3+
T CD8+PD-1+LAG3+
Cell type
T2–T1
T3–T1
T4–T1
Cell type
B cell
DC
MDSC
Monocyte
NK cell
T cell
UP - FDR < 0.1; P < 0.05
UP - FDR ≥ 0.1; P < 0.05
n.s. P > 0.05
DOWN - FDR ≥ 0.1; P < 0.05
DOWN - FDR < 0.1; P < 0.05
B
Monocyte
Mo
IMo
CMo DR+
Mo CD192+
Mo CD192+DR–
MoCX3CR1+
Dendritic cell
IMo CX3CR1+
CMo CX3CR1+
IMo CX3CR1+DR–
IMo CD192loCX3CR1dim
DC
DC CD16+
MDSC
PMN-MDSC
M-MDSC
PMN-MDSC LOX1+
NK cell
NK
NK CD56bright
NK CD56dim
Exhausted/hyperexhausted T cell
T CD8+LAG3
T CD8+TIM3+
T CD8+PD-1+LAG3+
T CD8+PD-1+TIM3+LAG3+
T LAG3+
Treg cell
Treg
Activated/effector T cell
T CX3CR1+
TEM PD-1+
T CD8+PD-1+
T CD8+CD28–PD-1+
TEM
T CD8+CD25+
T1 T2 T3 T4
C
MDSC
DC
B cell
Monocyte
NK cell
T cell
Activated/effector T-cell cluster
Exhausted T cell cluster
Rho
1
0.5
0
–0.5
–1
P value color
n.s. P > 0.05
FDR ≥ 0.1, P < 0.05
RDR < 0.1, P < 0.05
Type
Flow cytometry
RNA-seq
RNA-seq
DC
Eosinophils
Macrophages
Mast cell
Monocyte
Neutrophils
NK cell
T cell
aDC
pDC
NKT
CD4+ Tem
CD4+ Tcm
CD8+ Tem
CD8+ Tcm
Th1 cells
D
PMN-MDSC LOX1
R = –0.4
P = 0.013
CD8+ T cells
TEM PD-1+
R = 0.39
P = 0.016
Th1 cells
T CD8+PD-1+LAG3+
R = –0.49
P = 0.002
Th1 cells
TEM
R = 0.47
P = 0.003
CD8+ Tem
T CD8+PD-1+TIM3+LAG3+
R = –0.39
P = 0.015
CD8+ Tcm

$CD8^+PD\text{-}1^+TIM3^+LAG3^+$) or immunosuppressive myeloid cell subsets (e.g., PMN-MDSC-$LOX1^+$; Fig. 5C and D).

DISCUSSION

We have shown that a severely calorie-restricted, low-carbohydrate, low-protein, five-day dietary regimen that mimics fasting is safe and feasible when repeated every 21 to 28 days in combination with standard antitumor treatments, and it reshapes systemic metabolism and antitumor immunity in patients with cancer.

The incidence of G3/G4 FMD-related AEs was 12.9%, which allowed us to reject the null hypothesis that the real incidence is 20%, a threshold that we considered clinically significant to proceed with further investigation of the FMD. Of note, this threshold is significantly lower than that reported in recent clinical trials evaluating different types of innovative targeted therapies and immunotherapy strategies that received approval by regulatory agencies in the United States and in Europe (24–26). In addition, because several AEs attributed to the FMD (e.g., fatigue, nausea) can be also caused by concomitant anticancer treatments (e.g., ChT), the reported incidence of G3/G4 FMD-related AEs may represent an overestimation of the real incidence.

In parallel with good safety profile, the FMD was shown to be feasible, with a global compliance rate of 91.8% when considering all FMD cycles, and with major deviations reported only during 1.6% of FMD cycles. These data are especially relevant in light of the recently published trial "DIRECT," which investigated the antitumor activity of cyclic FMD in combination with neoadjuvant ChT in patients with $HER2^-$ breast cancer. Unfortunately, the study was prematurely interrupted due to poor patient adherence to the proposed experimental diet, and also because the FMD failed to reduce ChT-induced adverse events (7, 27). Despite longer duration (5 vs. 4 days) and more severe average daily calorie restriction [360 Kcal/day (range 300–600 Kcal/day) vs. 450 KCal/day (range: 200–1,200 Kcal/day)] of our FMD regimen (Supplementary Table S1) when compared with the FMD kit used in the DIRECT study, patient compliance with the FMD was better and the median number of completed FMD cycles was higher (4 vs. 2) in the NCT03340935 trial. This could be in part attributable to the differences in patient management, which included multidisciplinary team evaluation before each FMD cycle and daily e-mail/phone contact guaranteed by physicians to patients 24 hours a day during the FMD, or in FMD composition, including additional dietary options that patients could select according to their preferences (Supplementary Table S1; ref. 27). Because patient compliance with the FMD is an essential prerequisite for any desirable biological (e.g., metabolic, immunologic) and antitumor effect (as also suggested by subgroup analyses of the DIRECT study; ref. 7), the safety and feasibility of our FMD regimen makes it a good candidate regimen for future clinical studies.

One major issue related to the use of fasting/FMD in patients with cancer is the risk of causing progressive weight loss by inducing or accelerating the release of amino acids, glycerol, and fatty acids from skeletal muscles and adipose tissue (28). For this reason, patients who were underweight, or at higher risk to become malnourished, were excluded from enrollment. With these selection criteria, only 4% of patients discontinued the FMD due to progressive BMI reduction, and we observed restoration of baseline BMI in patients who completed at least three FMD cycles. These results indicate that the FMD is unlikely to cause progressive weight loss if patients are properly selected and strict discontinuation rules are used in the case of insufficient weight recovery.

Preclinical evidence in tumor-bearing mice suggests that fasting/FMD-induced reduction of blood glucose and insulin/IGF1 concentration (by approximately 30%–50%) is crucial in mediating its anticancer effects, either direct or immune-mediated (2, 5, 6, 29). Because of the complexity of homeostatic mechanisms regulating systemic metabolism in humans, such as glycerol- or amino acid–sustained neoglucogenesis, we expected less significant metabolic changes in patients than in mice (7, 30–32). Nevertheless, our experimental FMD regimen reduced median blood glucose, insulin, and IGF1 concentration by 18.6%, 50.7%, and 30.3%, respectively, that is, more than 1 to 3 days of water-only fasting (31, 33). Notably, these changes were independent of the type of primary tumor and concomitant anticancer therapy, and were consistently reproduced across subsequent FMD cycles, thus excluding the occurrence of systemic metabolic adaptation. Together, our data indicate that a well-tolerated FMD regimen results in metabolic changes that are qualitatively and quantitatively similar to metabolic modifications that are responsible for the anticancer effects of fasting/FMD in tumor-bearing mice (6, 29). We also showed that FMD-induced reduction of serum IGF1 levels is associated with the downregulation of total and activated IGF1R at the tumor level, thus providing first evidence of "pharmacodynamic" activity of FMD in human cancers. This result paves the way for combining the FMD with inhibitors of different nodes of the IGF1R/PI3K/AKT/mTORC1 axis in future clinical trials.

The most biologically novel and translationally relevant finding of this study consists in the broad immunomodulatory effects of the FMD at both systemic and tumor level. In the blood of patients with cancer and healthy volunteers, the FMD reduced total monocytes and several populations of immunosuppressive cells, such as M-MDSCs, PMN-MDSCs, and Tregs, while it increased cytotoxic T lymphocytes and cytolytic NK cells, and promoted a switch of $CD8^+$ cells toward an activated/memory phenotype. These changes were paralleled by similar and desirable immunologic modifications at the tumor level, where five-day fasting/FMD in patients with breast cancer increased total and activated intratumor $CD8^+$ T cells, aDCs, NK cells, and Tem cells, and it resulted in an enrichment of immune signatures previously associated with good prognosis and/or better response to therapies in patients with cancer. While recapitulating and expanding data previously published in tumor-bearing mice (3, 5, 34), our results provide first evidence that five-day FMD produces systemic immunologic effects that are associated with the activation of several antitumor immune programs at the tumor level in human cancers. In addition, some FMD-induced systemic immunologic modifications, such as the modulation of monocyte, MDSC, and NK cells, are long-lasting, that is, they are maintained at least 40 days after the end of FMD. These data indicate potential carryover immunologic effects of the FMD, and suggest that

in specific clinical contexts (e.g., less advanced tumors, combination with immune checkpoint inhibitors), a few FMD cycles could be sufficiently potent to stably reshape systemic immunity, thus determining the conditions for long-term synergistic antitumor effects of FMD and standard antitumor treatments.

Because IL6 plays an important role in the pathogenesis of cachexia (28), FMD-induced upregulation of the IL6/SOCS3/LIF signature at the tumor level may raise concerns about a potential cachexia-inducing effect of the FMD. However, the following arguments tend to exclude this hypothesis: (i) in this study, the FMD reduced, rather than increasing, blood IL6 (Fig. 2I); (ii) patients able to complete at least three FMD cycles maintained their weight stably over subsequent FMD cycles (Fig. 1G–I); (iii) in a previously published study by Caffa and colleagues in collaboration with our group, a less calorie-restricted FMD regimen did not cause meaningful changes in body composition, and in particular it did not cause sarcopenia (6); (iv) the observed increase in the transcription of *IL6* and *SOCS3* genes at the tumor level might more likely reflect the induction of the IFNG.GS (Fig. 4A and B), which promotes antitumor immunity.

In the perspective of achieving the desired biological effects (i.e., metabolic, immunomodulatory), defining the optimal duration of calorie-restricted regimens, such as fasting and FMD approaches, is a critical and still open issue. In the recently published study by Jordan and colleagues (35), a shorter fasting regimen (19 hours) resulted in a significant reduction of peripheral blood $CD14^+$ and $CD16^+$ monocytes in 12 healthy human volunteers. While these data are in line with the reduction of peripheral blood $CD14^+$ cells that we observed with our FMD regimen in both healthy volunteers and in patients with cancer, it remains unclear whether fasting/FMD regimens of shorter duration (e.g., 19 hours) can recapitulate the broad reshaping of systemic and, more importantly, intratumor immunity that we reported in this study.

Published preclinical studies, along with FMD-induced metabolic modifications (Fig. 1D–F), provide potential mechanistic explanations to the observed immunomodulatory effects. In 4T1 and Py8119 TNBC cell mouse transplants, glycolysis inhibition prevented G-CSF and GM-CSF production by cancer cells, thus reducing MDSC mobilization and their recruitment to the tumor site (36). More recently, short-term fasting was shown to downmodulate monocytes in peripheral blood and spleen of healthy mice by inhibiting systemic CCL2 production (35). In line with these data, our observation that the FMD lowers G-CSF, IL6, and CCL2 blood concentration in patients with supports the hypothesis that fasting/FMD-induced reduction of glycemia indirectly inhibits the egress of monocytes and MDSCs from the bone marrow and their accumulation in peripheral blood (Supplementary Fig. S16). In parallel, FMD-induced reduction of blood glucose and IGF1 concentration could in part explain the observed reduction of Tregs, whose proliferation and immune-suppressive functions were previously shown to depend on glucose and IGF1 availability (Supplementary Fig. S16; refs. 37, 38). On the other hand, the increment of activated $CD8^+$ T cells, NK cells, and Tem cells could indirectly result from relieved myeloid cell– or Treg cell–mediated immunosuppression (35, 39), or be the direct consequence of fasting/FMD–induced impairment of tumor glycolysis and microenvironment acidification (40–42), reduced blood IGF1 levels (5), or glucocorticoid-induced relocalization of memory T cells (43). In parallel, the observed increase in tumor-infiltrating activated/cytotoxic $CD8^+$ T cells could be in part mediated by FMD-induced increase in intratumor expression of *CCL3L1*, *CCL4L2*, *CCL5*, and *CX3CL1* genes, which encode ligands of CCR5 and CX3CR1 receptors (44–47), whose expression was increased in $CD8^+$ T cells collected after the FMD (Fig. 5A), or by downregulation of intratumor IGF1R, which has been recently shown to crucially contribute to the antitumor activity of immune checkpoint inhibitors (Supplementary Fig. S16; ref. 5).

Preclinical studies showed that restricting the dietary intake of carbohydrates or proteins affects the frequency/activation status of myeloid and lymphoid cells in peripheral organs and at the tumor level (35, 36, 48, 49). Because our FMD regimen is characterized by a severe restriction of both carbohydrates and proteins, the observed immunomodulatory effects could result from a combination of (i) carbohydrate restriction–induced reduction of blood glucose and CCL2, G-CSF, and GM-CSF levels, with consequently impaired monocyte mobilization from the bone marrow (35, 36); (ii) increased blood concentration of ketone bodies, which downmodulate PD-L1 expression in monocytes, thus inhibiting their immunosuppressive properties (34); (iii) protein restriction–induced reduction of blood IGF1 levels and inhibition of IGF1/IGFR1/PI3K/AKT/mTORC1 axis in cancer cells, myeloid cells, or Tregs, with the consequent activation of intratumor effector cells and memory T cells (5, 37, 38, 48). Future clinical trials will clarify which dietary components or FMD-induced metabolic changes are responsible for the observed modifications of individual immune cell populations.

In conclusion, cyclic FMD is a safe, feasible, and inexpensive dietary intervention that modulates systemic metabolism and boosts antitumor immunity in patients with cancer. Our study lays the foundations for recently initiated phase II clinical trials (e.g., NCT03709147, NCT04248998, NCT03700437) that are investigating the anticancer activity/efficacy of cyclic FMD in combination with ChT, target therapy, or immunotherapy.

METHODS

Clinical Study Procedures

NCT03340935 (https://clinicaltrials.gov/ct2/show/NCT03340935) is a single-arm, prospective clinical trial, in which all enrolled patients received experimental FMD in combination with their standard-of-care treatments. NCT03454282 (https://clinicaltrials.gov/ct2/show/NCT03454282) is a single-arm, prospective trial in which enrolled patients undergo five-day FMD before surgery without any concomitant antitumor therapies. Therefore, no randomization procedures were used to allocate patients to different treatment arms, and the studies were not blinded. Details regarding sample size calculation, study hypotheses/objectives, and power analysis can be found in the sections below. The main clinical characteristics of patients enrolled in the NCT03340935 and NCT03454282 trials, including age, sex, tumor type, tumor stage, and concomitant therapies, are summarized in Table 1 and Supplementary Table S6, respectively. INT 79/17 was

a prospective, observational study. The main clinical characteristics of patients enrolled in the INT 79/17 study are summarized in Supplementary Table S3.

Clinical studies were conducted in accordance with the Declaration of Helsinki and the principles of Good Clinical Practice. The Institutional Review Board (IRB) and the Ethics Committee of Fondazione IRCCS Istituto Nazionale dei Tumori di Milano approved the NCT03340935 trial (INT 10/17), the NCT03454282 trial (INT 157/17) and the observational study (INT 79/17). All patients provided written informed consent for enrollment in these studies, before any study-related procedures, as well as for the use of clinical and biological data for research purposes.

NCT03340935 Trial

Study Design and Objectives. NCT03340935 was a monocentric, open label, single-arm, prospective clinical trial aimed at evaluating the safety, feasibility, metabolic, and immunomodulatory effects of cyclic FMD in patients with different cancer types, disease stages, and receiving different types of standard antitumor treatments.

Study Objectives and Sample Size Calculation. The primary objective of the study was to assess the incidence of severe, G3/G4 AEs related to the FMD. The null hypothesis that the true rate of G3/G4 FMD-related AEs rate is 20% was tested against a one-sided alternative hypothesis. We used a two-stage Green–Dahlberg design (50). Details about the two-stage approach used and the sample size calculation are described in the Supplementary Methods. Secondary objectives of the study were to investigate: (i) the feasibility of the FMD, as defined as patient ability to be compliant with the prescribed regimen; (ii) short-term (before vs. after FMD; see Fig. 1A) and long-term (across subsequent FMD cycles) modifications of metabolic blood parameters; (iii) short- and long-term modifications of patient BMI.

In a subgroup of 38 patients consenting to undergo additional biological evaluations before and after the FMD, we assessed through multicolor flow cytometry analysis the impact of the FMD on specific PBMC populations. Patient selection criteria and the description of the control groups are detailed in the Supplementary Methods.

FMD Regimen and Patient Management. All patients enrolled were prescribed the same FMD regimen, consisting in a five-day, plant-based, calorie-restricted (up to 600 Kcal on day 1; up to 300 Kcal on days 2, 3, 4, and 5), low-carbohydrate, low-protein diet (Fig. 1A). The experimental dietary regimen was prescribed as a list of foods and beverages, with their maximum allowed amount (in grams and liters, respectively) clearly specified (Supplementary Table S1). See the Supplementary Methods for more details about the FMD regimen, patient management, analysis of patient compliance, incidence, and grading of FMD-related AEs and metabolic analyses.

Immunologic Analyses. In a subgroup of 38 patients, an additional amount of peripheral blood (15 mL) was obtained before FMD initiation and at the end of the FMD for immunologic analyses. PBMCs were also analyzed in: (i) a cohort of 8 healthy subjects undergoing blood sampling (15 mL) before initiating the FMD and at the end of the FMD; (ii) a cohort 13 patients with advanced breast cancer (Supplementary Table S3) who refused to be enrolled in the NCT03340935 trial, and were enrolled in a prospective observational study (INT 79/17) in which they underwent blood collection and metabolic/immunologic evaluations two days before ChT administration and three days after ChT, that is, similarly to patients undergoing the FMD in combination with ChT.

Gating strategies for myeloid and lymphoid cells are depicted in Supplementary Fig. S4A–S4F. Fluorescence Minus One (FMO) samples were used as controls (Supplementary Fig. S4G). See Supplementary Methods for more details about PBMC isolation, staining procedures, and details on myeloid cells, MDSC subsets, and lymphoid populations analyzed.

Selected cytokines and chemokines were detected in plasma samples from 34 patients (see Supplementary Methods). The complete list of antibodies and other reagents is provided in Supplementary Table S17.

DigesT (NCT03454282) Trial

Study Design. DigesT (NCT03454282) is a window-of-opportunity clinical trial aimed at investigating the impact of five-day FMD on systemic and intratumor immunity in patients with surgically resectable breast cancer or melanoma. Patients enrolled in the DigesT study initiate the FMD 12–15 days before surgery. The FMD regimen used in the DigesT trial is the same that has been tested in the NCT03340935 trial (Supplementary Table S1).

Metabolic and Other Biochemical Analyses. Patients underwent blood and urine sampling after at least 8-hour complete fasting on the morning of FMD initiation (T1), on the morning of FMD completion (T2), the day of surgery (T3), and approximately 30 days after surgery (T4; Fig. 3A). We reported data about plasma glucose, serum insulin, and IGF1 and urinary ketone bodies.

Transcriptomic Analysis in Breast Cancer Specimens. In this study, we reported results of an unplanned, interim analysis of global gene expression profiles in 22 paired FFPE tumor tissue specimens collected before the FMD (diagnostic biopsies) and after the FMD (surgical tumor specimens) from 22 patients with consecutive breast cancer for whom a sufficient amount and quality of tumor tissue was available for RNA-seq and IHC analyses (Supplementary Fig. S7). For details about RNA extraction, RNA-seq libraries' preparation, differential gene expression, and pathway analyses see the Supplementary Methods.

IHC Analysis. In the same 22 paired tumor specimens, we assessed by IHC the presence of tumor-infiltrating $CD8^+$ T lymphocytes, $CD68^+$ cells, Perforin 1, Granzyme B, IGF1R, and phospho-IGF1R. See the Supplementary Methods for the details about IHC procedures.

PBMC Analyses. In a subgroup of 19 of 22 DigesT patients, we collected 15 mL of peripheral blood at the end of the FMD (T2) and at subsequent time points (T3: surgery, occurring 7–10 days after the end of the FMD; T4: ~30 days after surgery) for high-dimensional flow cytometry analysis of PBMCs. The immune cell subsets captured by this analysis, as well as the gating strategy of the main populations, are depicted in Supplementary Figs. S11A, S11B, S12, and S13. See Supplementary Methods for more details about PBMC isolation and the staining procedures. The complete list of flow cytometry antibodies and other reagents is provided in Supplementary Table S18.

Statistical Analysis

The paired Wilcoxon test was used to assess changes in BMI, metabolic, and immunologic parameters before and after FMD in patients with cancer, as well as BMI measurements before consecutive FMD cycles. Patient BMI and metabolic parameters were illustrated through box plots showing median values, with the boundaries of the rectangle representing the first and third quartiles, while whiskers extend to the extreme data points that are no more than 1.5 times the interquartile range. Frequencies of immune cell populations in PBMCs and tumor specimens, the concentration of plasmatic cytokines/chemokines, quantifications of tumor proteins by IHC, and the expression of intratumor genes were illustrated through box plots and through dot plots indicating parameter values in each patient before and at different time points after the FMD.

A significance threshold of 0.05 was used for all statistical tests. The *P* value for the indicated statistical test is reported for each comparison in each figure. All statistical analyses and graphs were performed with the software R.

Data Availability

RNA-seq data are deposited on the European Genome-Phenome Archive (EGA) under accession number EGAS00001004944. Other data generated in this study are available upon request from the corresponding author.

Authors' Disclosures

C. Vernieri reports grants from AIRC (Associazione Italiana per la Ricerca sul Cancro) during the conduct of the study; in addition, C. Vernieri has a patent for PCT/IB2020/055956 pending and a patent for PCT/IT2020/000083 pending. V. Huber reports grants from Associazione Italiana per la Ricerca sul Cancro (AIRC IG25078) during the conduct of the study. M.C. Garassino reports grants and personal fees from Astra Zeneca, Merck; personal fees from BMS, Roche, Daiichi Sankyo, Celgene, GSK, Eli Lilly, Novartis, and personal fees from Regerenon during the conduct of the study. G. Bianchi reports personal fees from Novartis, Eli Lilly, and personal fees from Roche outside the submitted work. S. Minucci reports a patent for PCT/EP2018/063257 pending. V.D. Longo reports non-financial support and other support from L nutra during the conduct of the study; other support from L nutra outside the submitted work; in addition, V.D. Longo has a patent for several patents related to this topic, but not based on this trial, pending. G. Pruneri reports personal fees from Roche Foundation One, Bayer, Novartis, and personal fees from Lilly outside the submitted work. D. Bedognetti reports grants from Sidra Medicine during the conduct of the study. L. Rivoltini reports grants from Associazione Italiana per la Ricerca sul Cancro (AIRC) (IG-2017 no. 20752) and grants from European Community - Horizon 2020 Precious Grant Agreement number 686089 during the conduct of the study; in addition, L. Rivoltini has a patent for FMD regimen pending. F. de Braud reports a patent for PCT/IB2020/055956 pending and a patent for IT201900009954 pending; and Roche, EMD Serono, NMS Nerviano Medical Science, Sanofi, MSD, Novartis, Incyte, BMS, Menarini Healthcare Research & Pharmacoepidemiology, Merck Group, Pfizer, Servier, AMGEN, Incyte. No disclosures were reported by the other authors.

Authors' Contributions

C. Vernieri: Conceptualization, resources, data curation, formal analysis, supervision, funding acquisition, validation, investigation, visualization, methodology, writing–original draft, project administration, writing–review and editing. **G. Fucà:** Data curation, formal analysis, investigation, writing–review and editing. **F. Ligorio:** Data curation, investigation, writing–review and editing. **V. Huber:** Investigation, writing–review and editing. **A. Vingiani:** Formal analysis, investigation, writing–original draft. **F. Iannelli:** Formal analysis, methodology, writing–review and editing. **A. Raimondi:** Data curation, investigation, writing–review and editing. **D. Rinchai:** Formal analysis, investigation, writing–review and editing. **G. Frigè:** Investigation, writing–review and editing. **A. Belfiore:** Investigation, writing–review and editing. **L. Lalli:** Investigation, writing–review and editing. **C. Chiodoni:** Validation, investigation, writing–review and editing. **V. Cancila:** Investigation, writing–review and editing. **F. Zanardi:** Formal analysis, writing–review and editing. **A. Ajazi:** Investigation, writing–review and editing. **S. Cortellino:** Investigation, writing–review and editing. **V. Vallacchi:** Investigation, writing–review and editing. **P. Squarcina:** Investigation, writing–review and editing. **A. Cova:** Investigation, writing–review and editing. **S. Pesce:** Investigation, writing–review and editing. **P. Frati:** Investigation, writing–review and editing. **R. Mall:** Writing–review and editing. **P.A. Corsetto:** Investigation, writing–review and editing. **A.M. Rizzo:** Investigation, writing–review and editing. **C. Ferraris:** Investigation, writing–review and editing. **S. Folli:** Investigation, writing–review and editing. **M.C. Garassino:** Investigation, writing–review and editing. **G. Capri:** Investigation, writing–review and editing. **G. Bianchi:** Investigation, writing–review and editing. **M.P. Colombo:** Resources, investigation, Writing–review and editing. **S. Minucci:** Investigation, writing–review and editing. **M. Foiani:** Investigation, writing–review and editing. **V.D. Longo:** Resources, investigation, writing–review and editing. **V. Torri:** Formal analysis, methodology, writing–review and editing. **G. Pruneri:** Resources, investigation, methodology, writing–review and editing. **D. Bedognetti:** Formal analysis, investigation, visualization, methodology, writing–original draft, writing–review and editing. **L. Rivoltini:** Resources, funding acquisition, investigation, visualization, methodology, writing–original draft, writing–review and editing. **F. de Braud:** Conceptualization, funding acquisition, investigation, project administration, writing–review and editing.

Acknowledgments

We thank the "Associazione Italiana per la Ricerca sul Cancro" (AIRC), the Scientific Directorate of Fondazione IRCCS Istituto Nazionale dei Tumori, the European Union Framework Program Horizon 2020 and the Italian Ministry of Health for funding our research. We thank Dr. Monica Milano for her help in writing the study protocol and we also thank healthy volunteers who underwent the FMD together with two authors of the article (C. Vernieri and G. Fucà). We thank Filippo Cascone, Greta Malena, Gloria Colangelo, Antonia Martinetti, and Lucrezia Zanenga for their help in biological sample collection and patient management. We especially thank all patients who took part in this clinical trial and their families. This work was supported by funds of the Scientific Directorate of Fondazione IRCCS Istituto Nazionale dei Tumori (Milan, Italy), by funds of the "Associazione Italiana per la Ricerca sul Cancro" (AIRC; IG-2017 no. 20752: principal investigator, L. Rivoltini; MFAG-2019 no. 22977: principal investigator: C. Vernieri) and the European Union Framework Program Horizon 2020 (TRANSCAN-2, code no. TRS-2016-00000393: principal investigator: F. de Braud) funded by the Italian Ministry of Health.

The costs of publication of this article were defrayed in part by the payment of page charges. This article must therefore be hereby marked *advertisement* in accordance with 18 U.S.C. Section 1734 solely to indicate this fact.

Received January 11, 2021; revised August 4, 2021; accepted October 22, 2021; published first November 17, 2021.

REFERENCES

1. Lee C, Raffaghello L, Brandhorst S, Safdie FM, Bianchi G, Martin-Montalvo A, et al. Fasting cycles retard growth of tumors and sensitize a range of cancer cell types to chemotherapy. Sci Transl Med 2012;4:124ra27.
2. Lee C, Safdie FM, Raffaghello L, Wei M, Madia F, Parrella E, et al. Reduced levels of IGF-I mediate differential protection of normal and cancer cells in response to fasting and improve chemotherapeutic index. Cancer Res 2010;70:1564–72.
3. Di Biase S, Lee C, Brandhorst S, Manes B, Buono R, Cheng CW, et al. Fasting-mimicking diet reduces HO-1 to promote T cell-mediated tumor cytotoxicity. Cancer Cell 2016;30:136–46.
4. Di Tano M, Raucci F, Vernieri C, Caffa I, Buono R, Fanti M, et al. Synergistic effect of fasting-mimicking diet and vitamin C against KRAS mutated cancers. Nat Commun 2020;11:2332.

5. Ajona D, S. O-E, Lozano T, Exposito F, Calvo A, Valencia K, et al. Short-term starvation reduces IGF-1 levels to sensitize lung tumors to PD-1 immune checkpoint blockade. Nat Cancer 2020;1:75–85.
6. Caffa I, Spagnolo V, Vernieri C, Valdemarin F, Becherini P, Wei M, et al. Fasting-mimicking diet and hormone therapy induce breast cancer regression. Nature 2020;583:620–4.
7. de Groot S, Lugtenberg RT, Cohen D, Welters MJP, Ehsan I, Vreeswijk MPG, et al. Fasting mimicking diet as an adjunct to neoadjuvant chemotherapy for breast cancer in the multicentre randomized phase 2 DIRECT trial. Nat Commun 2020;11:3083.
8. Bronte V, Brandau S, Chen SH, Colombo MP, Frey AB, Greten TF, et al. Recommendations for myeloid-derived suppressor cell nomenclature and characterization standards. Nat Commun 2016;7:12150.
9. Filipazzi P, Valenti R, Huber V, Pilla L, Canese P, Iero M, et al. Identification of a new subset of myeloid suppressor cells in peripheral blood of melanoma patients with modulation by a granulocyte-macrophage colony-stimulation factor-based antitumor vaccine. J Clin Oncol 2007;25:2546–53.
10. Roux C, Jafari SM, Shinde R, Duncan G, Cescon DW, Silvester J, et al. Reactive oxygen species modulate macrophage immunosuppressive phenotype through the up-regulation of PD-L1. Proc Natl Acad Sci U S A 2019;116:4326–35.
11. Moretta L. Dissecting CD56dim human NK cells. Blood 2010;116:3689–91.
12. Anderson AC, Joller N, Kuchroo VK. Lag-3, Tim-3, and TIGIT: co-inhibitory receptors with specialized functions in immune regulation. Immunity 2016;44:989–1004.
13. DeNardo DG, Brennan DJ, Rexhepaj E, Ruffell B, Shiao SL, Madden SF, et al. Leukocyte complexity predicts breast cancer survival and functionally regulates response to chemotherapy. Cancer Discov 2011;1:54–67.
14. Charoentong P, Finotello F, Angelova M, Mayer C, Efremova M, Rieder D, et al. Pan-cancer immunogenomic analyses reveal genotype-immunophenotype relationships and predictors of response to checkpoint blockade. Cell Rep 2017;18:248–62.
15. Aran D, Hu Z, Butte AJ. xCell: digitally portraying the tissue cellular heterogeneity landscape. Genome Biol 2017;18:220.
16. Benci JL, Johnson LR, Choa R, Xu Y, Qiu J, Zhou Z, et al. Opposing functions of interferon coordinate adaptive and innate immune responses to cancer immune checkpoint blockade. Cell 2019;178:933–48.
17. Condamine T, Dominguez GA, Youn JI, Kossenkov AV, Mony S, Alicea-Torres K, et al. Lectin-type oxidized LDL receptor-1 distinguishes population of human polymorphonuclear myeloid-derived suppressor cells in cancer patients. Sci Immunol 2016;1:aaf8943.
18. Krieg C, Nowicka M, Guglietta S, Schindler S, Hartmann FJ, Weber LM, et al. High-dimensional single-cell analysis predicts response to anti-PD-1 immunotherapy. Nat Med 2018;24:144–53.
19. Wang L, Simons DL, Lu X, Tu TY, Avalos C, Chang AY, et al. Breast cancer induces systemic immune changes on cytokine signaling in peripheral blood monocytes and lymphocytes. EBioMedicine 2020;52:102631.
20. Fromm PD, Silveira PA, Hsu JL, Papadimitrious MS, Lo TH, Ju X, et al. Distinguishing human peripheral blood CD16(+) myeloid cells based on phenotypic characteristics. J Leukoc Biol 2020;107:323–39.
21. Gerlach C, Moseman EA, Loughhead SM, Alvarez D, Zwijnenburg AJ, Waanders L, et al. The chemokine receptor CX3CR1 defines three antigen-experienced CD8 T cell subsets with distinct roles in immune surveillance and homeostasis. Immunity 2016;45:1270–84.
22. Yan Y, Cao S, Liu X, Harrington SM, Bindeman WE, Adjei AA, et al. CX3CR1 identifies PD-1 therapy-responsive CD8+ T cells that withstand chemotherapy during cancer chemoimmunotherapy. JCI Insight 2018;3:e97828.
23. Flippe L, Bezie S, Anegon I, Guillonneau C. Future prospects for CD8(+) regulatory T cells in immune tolerance. Immunol Rev 2019;292:209–24.
24. André F, Ciruelos E, Rubovszky G, Campone M, Loibl S, Rugo HS, et al. Alpelisib for PIK3CA-mutated, hormone receptor–positive advanced breast cancer. N Engl J Med 2019;380:1929–40.
25. Gandhi L, Rodríguez-Abreu D, Gadgeel S, Esteban E, Felip E, De Angelis F, et al. Pembrolizumab plus chemotherapy in metastatic non–small-cell lung cancer. N Engl J Med 2018;378:2078–92.
26. Cremolini C, Antoniotti C, Rossini D, Lonardi S, Loupakis F, Pietrantonio F, et al. Upfront FOLFOXIRI plus bevacizumab and reintroduction after progression versus mFOLFOX6 plus bevacizumab followed by FOLFIRI plus bevacizumab in the treatment of patients with metastatic colorectal cancer (TRIBE2): a multicentre, open-label, phase 3, randomised, controlled trial. Lancet Oncol 2020;21:497–507.
27. Vernieri C, Ligorio F, Zattarin E, Rivoltini L, de Braud F. Fasting-mimicking diet plus chemotherapy in breast cancer treatment. Nat Commun 2020;11:4274.
28. Argiles JM, Busquets S, Stemmler B, Lopez-Soriano FJ. Cancer cachexia: understanding the molecular basis. Nat Rev Cancer 2014;14:754–62.
29. Elgendy M, Ciro M, Hosseini A, Weiszmann J, Mazzarella L, Ferrari E, et al. Combination of hypoglycemia and metformin impairs tumor metabolic plasticity and growth by modulating the PP2A-GSK3beta-MCL-1 axis. Cancer Cell 2019;35:798–815.
30. Vernieri C, Casola S, Foiani M, Pietrantonio F, de Braud F, Longo V. Targeting cancer metabolism: dietary and pharmacologic interventions. Cancer Discov 2016;6:1315–33.
31. Dorff TB, Groshen S, Garcia A, Shah M, Tsao-Wei D, Pham H, et al. Safety and feasibility of fasting in combination with platinum-based chemotherapy. BMC Cancer 2016;16:360.
32. Bauersfeld SP, Kessler CS, Wischnewsky M, Jaensch A, Steckhan N, Stange R, et al. The effects of short-term fasting on quality of life and tolerance to chemotherapy in patients with breast and ovarian cancer: a randomized cross-over pilot study. BMC Cancer 2018;18:476.
33. de Groot S, Vreeswijk MP, Welters MJ, Gravesteijn G, Boei JJ, Jochems A, et al. The effects of short-term fasting on tolerance to (neo) adjuvant chemotherapy in HER2-negative breast cancer patients: a randomized pilot study. BMC Cancer 2015;15:652.
34. Ferrere G, Tidjani Alou M, Liu P, Goubet AG, Fidelle M, Kepp O, et al. Ketogenic diet and ketone bodies enhance the anticancer effects of PD-1 blockade. JCI Insight 2021;6:e145207.
35. Jordan S, Tung N, Casanova-Acebes M, Chang C, Cantoni C, Zhang D, et al. Dietary intake regulates the circulating inflammatory monocyte pool. Cell 2019;178:1102–14.
36. Li W, Tanikawa T, Kryczek I, Xia H, Li G, Wu K, et al. Aerobic glycolysis controls myeloid-derived suppressor cells and tumor immunity via a specific CEBPB isoform in triple-negative breast cancer. Cell Metab 2018;28:87–103.
37. De Rosa V, Galgani M, Porcellini A, Colamatteo A, Santopaolo M, Zuchegna C, et al. Glycolysis controls the induction of human regulatory T cells by modulating the expression of FOXP3 exon 2 splicing variants. Nat Immunol 2015;16:1174–84.
38. Bilbao D, Luciani L, Johannesson B, Piszczek A, Rosenthal N. Insulin-like growth factor-1 stimulates regulatory T cells and suppresses autoimmune disease. EMBO Mol Med 2014;6:1423–35.
39. Newton R, Priyadharshini B, Turka LA. Immunometabolism of regulatory T cells. Nat Immunol 2016;17:618–25.
40. Brand A, Singer K, Koehl GE, Kolitzus M, Schoenhammer G, Thiel A, et al. LDHA-associated lactic acid production blunts tumor immunosurveillance by T and NK cells. Cell Metab 2016;24:657–71.
41. Ho PC, Bihuniak JD, Macintyre AN, Staron M, Liu X, Amezquita R, et al. Phosphoenolpyruvate is a metabolic checkpoint of anti-tumor T cell responses. Cell 2015;162:1217–28.
42. Cascone T, McKenzie JA, Mbofung RM, Punt S, Wang Z, Xu C, et al. Increased tumor glycolysis characterizes immune resistance to adoptive T cell therapy. Cell Metab 2018;27:977–87.
43. Collins N, Han SJ, Enamorado M, Link VM, Huang B, Moseman EA, et al. The bone marrow protects and optimizes immunological memory during dietary restriction. Cell 2019;178:1088–101.
44. Mlecnik B, Tosolini M, Charoentong P, Kirilovsky A, Bindea G, Berger A, et al. Biomolecular network reconstruction identifies T-cell homing factors associated with survival in colorectal cancer. Gastroenterology 2010;138:1429–40.

45. Bedognetti D, Spivey TL, Zhao Y, Uccellini L, Tomei S, Dudley ME, et al. CXCR3/CCR5 pathways in metastatic melanoma patients treated with adoptive therapy and interleukin-2. Br J Cancer 2013;109:2412–23.
46. Litchfield K, Reading JL, Puttick C, Thakkar K, Abbosh C, Bentham R, et al. Meta-analysis of tumor- and T cell-intrinsic mechanisms of sensitization to checkpoint inhibition. Cell 2021;184:596–614.
47. Galon J, Angell HK, Bedognetti D, Marincola FM. The continuum of cancer immunosurveillance: prognostic, predictive, and mechanistic signatures. Immunity 2013;39:11–26.
48. Orillion A, Damayanti NP, Shen L, Adelaiye-Ogala R, Affronti H, Elbanna M, et al. Dietary protein restriction reprograms tumor-associated macrophages and enhances immunotherapy. Clin Cancer Res 2018;24:6383–95.
49. Rubio-Patino C, Bossowski JP, De Donatis GM, Mondragon L, Villa E, Aira LE, et al. Low-protein diet induces IRE1alpha-dependent anticancer immunosurveillance. Cell Metab 2018;27:828–42.
50. Green SJ, Dahlberg S. Planned versus attained design in phase II clinical trials. Stat Med 1992;11:853–62.